

Wright State University

CORE Scholar

[Browse all Theses and Dissertations](#)

[Theses and Dissertations](#)

2022

Has Winter Weather in Southwest Ohio Been Affected by the El Niño Southern Oscillation, the North Atlantic Oscillation, the Pacific Decadal Oscillation, and the Atlantic Multidecadal Oscillation?

John A. Blue
Wright State University

Follow this and additional works at: https://corescholar.libraries.wright.edu/etd_all



Part of the [Earth Sciences Commons](#), and the [Environmental Sciences Commons](#)

Repository Citation

Blue, John A., "Has Winter Weather in Southwest Ohio Been Affected by the El Niño Southern Oscillation, the North Atlantic Oscillation, the Pacific Decadal Oscillation, and the Atlantic Multidecadal Oscillation?" (2022). *Browse all Theses and Dissertations*. 2591.
https://corescholar.libraries.wright.edu/etd_all/2591

This Thesis is brought to you for free and open access by the Theses and Dissertations at CORE Scholar. It has been accepted for inclusion in Browse all Theses and Dissertations by an authorized administrator of CORE Scholar. For more information, please contact library-corescholar@wright.edu.

HAS WINTER WEATHER IN SOUTHWEST OHIO BEEN AFFECTED BY THE EL NINO
SOUTHERN OSCILLATION, THE NORTH ATLANTIC OSCILLATION, THE PACIFIC
DECADAL OSCILLATION, AND THE ATLANTIC MULTIDECADAL OSCILLATION?

A Thesis submitted in partial fulfillment of the
requirements for the degree of
Master of Science

by

JOHN A. BLUE

B.S., Wright State University, 2020

2022

Wright State University

WRIGHT STATE UNIVERSITY
GRADUATE SCHOOL

April 22, 2022

I HEREBY RECOMMEND THAT THE THESIS PREPARED UNDER MY SUPERVISION BY John A. Blue ENTITLED Has Winter Weather in Southwest Ohio Been Affected by the El Niño Southern Oscillation, the North Atlantic Oscillation, the Pacific Decadal Oscillation, and the Atlantic Multidecadal Oscillation? BE ACCEPTED IN PARTIAL FULFILLMENT OF THE REQUIREMENTS FOR THE DEGREE OF Master of Science.

Robert W. Ritzi Jr., Ph.D.
Thesis Director

Rebecca E. Teed, Ph.D.
Chair, Department of Earth &
Environmental Sciences

Committee on Final Examination:

Robert W. Ritzi Jr., Ph.D.

Christopher C. Barton, Ph.D.

Abinash Agrawal, Ph.D.

Barry Milligan, Ph.D.
Vice Provost for Academic Affairs
Dean of the Graduate School

ABSTRACT

Blue, John A., M.S., Department of Earth & Environmental Science, Wright State University, 2022. Has Winter Weather in Southwest Ohio Been Affected by the El Niño Southern Oscillation, the North Atlantic Oscillation, the Pacific Decadal Oscillation, and the Atlantic Multidecadal Oscillation?

Winter temperature and precipitation in Southwest Ohio over the last century were examined for anomalies attributable to teleconnections with large-scale atmospheric perturbations caused by the El Niño Southern Oscillation (ENSO), the North Atlantic Oscillation (NAO), the Pacific Decadal Oscillation (PDO), and the Atlantic Multidecadal Oscillation (AMO). The record of temperature gives evidence of a teleconnection with the NAO, ENSO, and PDO, with the strongest link being for phases of the NAO. Most winters during positive NAO phases had mean monthly temperature warmer than the century long mean, and the majority of negative NAO phase winters had colder temperatures. The difference in average temperature between positive and negative NAO phase winters was 0.82°C and is statistically significant at the $p=0.0005$ level. Winters were also increasingly warmer when NAO was increasingly positive, and increasingly colder when NAO was increasingly negative (regression-model with $p=E-5$). The support for this teleconnection was the strongest when NAO is out of phase with ENSO and PDO. For example, the 21 winters when the NAO phase was positive and ENSO and PDO phases were negative (condition A) were 1.73°C warmer on average than the 12 winters when NAO was negative and ENSO and PDO were positive (condition B), and the difference is statistically significantly different at the $p=0.02$ level. The warmest winters on record (mean-monthly temperature of 6.9°C) occurred under condition A, while the coldest (5.2°C) occurred under condition B. The NAO, ENSO and PDO variations explain 0.25 of the overall variance in mean winter temperature (multi-regression-model with $p=3.5E-05$). The record does not give

statistical support for an influence on winter temperature by the AMO. The record gives statistical support for a smaller influence of NAO, ENSO, PDO, and AMO phases on precipitation, with the phases explaining 7% of the variance in winter precipitation (multi-regression model with $p=0.018$).

TABLE OF CONTENTS

I.	INTRODUCTION	1
II.	BACKGROUND AND PREVIOUS WORK	5
	A. JET STREAMS AND THE POLAR VORTEX	5
	B. EL NINO SOUTHERN OSCILLATION (ENSO)	8
	C. PACIFIC DECADEAL OSCILLATION (PDO)	13
	D. NORTH ATLANTIC OSCILLATION (NAO)	16
	E. ATLANTIC MULTIDECADAL OSCILLATION (AMO)	18
	F. INTERACTIONS BETWEEN ENSO, PDO, NAO, AND AMO	20
III.	DATA AND METHODS	22
	A. DATA	22
	B. METHODS.....	24
	B.1. TESTING HYPOTHESES FOR ANOMALIES CAUSED BY PERTURBATIONS INDIVIDUALLY	24
	B.1.A. PROPORTION OF POSITIVE PHASE WINTERS WITH TEMPERATURE OR PRECIPITATION ABOVE OR BELOW NEGATIVE PHASE WINTERS	25
	B.1.B. INDEPENDENT SAMPLE T-TESTS COMPARISON OF THE MEAN WINTER VALUES BETWEEN POSITIVE AND NEGATIVE PHASE INDICES.....	25
	B.1.C. SIMPLE LINEAR REGRESSION.....	25
	B.2. TESTING HYPOTHESES FOR ANOMALIES CAUSE BY THE COMBINED INFLUENCE OF PERTURBATIONS.....	26
	B.2.A. MULTIPLE LINEAR REGRESSION WITHOUT INTERACTIONS	26
	B.2.B. MULTIPLE LINEAR REGRESSION WITH INTERACTIONS.....	27
IV.	RESULTS FOR TEMPERATRE	28
	A. ANALYSIS OF SAMPLE PROPORTIONS AND DIFFERENCES IN MEANS AMONG EACH POSITIVE AND NEGATIVE PHASES.....	28
	B. SEPARATE REGRESSION ON EACH INDEX	31
	C. MULTIPLE REGRESSION WITH FOUR INDICES	32
	D. MULTIPLE REGRESSION WITH FOUR INDICES AND INTERACTIONS.....	33
V.	RESULTS FOR PRECIPITATION	40
	A. ANALYSIS OF SAMPLE PROPORTIONS AND DIFFERENCES IN MEANS AMONG EACH POSITIVE AND NEGATIVE PHASES.....	40
	B. SEPARATE REGRESSION ON EACH INDEX	42
	C. MULTIPLE REGRESSION WITH FOUR INDICES	43
	D. MULTIPLE REGRESSION WITH FOUR INDICES AND INTERACTIONS.....	44
VI.	DISCUSSION	46
	A. TEMPERATURE	46
	B. PRECIPITATION.....	48
	C. IMPLICATIONS	49
	D. FUTURE WORK	49
VII.	CONCLUSIONS	51
	REFERENCES	53

LIST OF FIGURES

Figure 1. Southwest Ohio study area with data location	2
Figure 2. Indices representing four types of global perturbations	3
Figure 3. Idealized model of the three-fold structure of the tropopause	6
Figure 4. Difference between the polar vortex and polar jet stream, and how they are related ...	7
Figure 5. Composite maps of sea-surface temperature anomalies for El Niño and La Niña	10
Figure 6. Expected weather effects related to jet stream position during ENSO phases	11
Figure 7. Examples of linear regression for precipitation and temperature vs. MEI	12
Figure 8. Composite maps of sea surface temperature for different PDO and ENSO phases	13
Figure 9. Correlation between precipitation anomalies for both PDO and ENSO	15
Figure 10. Composite maps of winter geopotential heights/anomalies for NAO phases	17
Figure 11. Expected weather effects and jet stream positions related to NAO phases	18
Figure 12. Mean SST anomaly map for warm AMO years	19
Figure 13. Hypothesized temperature affects for each positive and negative phase index	21
Figure 14. Records for winter weather at Urbana station	24
Figure 15. Linear regressions for each index individually against each temperature metric	32
Figure 16. Three-way interaction model for the mean monthly temperature metric	35
Figure 17. Mean monthly temperature from 1901 to 2016 for combinations 4, 6, and 8	37
Figure 18. Linear regressions for each index individually against each precipitation metric	43

LIST OF TABLES

Table 1. Results from linear regression for USHCN data	12
Table 2. Hypotheses for each perturbations effect on winter weather in Southwest Ohio	21
Table 3. Summary statistics for metrics on winter weather for each perturbation	23
Table 4. Sample proportions results of positive and negative phase indices for temperature	29
Table 5. Results for the differences in the means among positive and negative phases indices...	30
Table 6. Temperature regression, results with each individual index on each metric	31
Table 7. Multiple regression for each metric without considering interaction terms on temp	33
Table 8. Multiple regression for each metric with all 1, 2, and 3-way interaction terms	34
Table 9. Eight combinations of index states for NAO, PDO, and MEI	36
Table 10. Statistics for monthly winter temp for years under each combination in Table 9	36
Table 11. Proportions of combinations 4, 6, and 8 with mean temp above/below winter mean ..	38
Table 12. Results from hypothesis testing on differences in the mean	38
Table 13. Multiple comparison between combinations	39
Table 14. Sample proportions results of positive and negative phase indices for precipitation ...	40
Table 15. Results for differences in the means among positive and negative phases indices	41
Table 16. Precipitation regression, results with each individual index on each metric	42
Table 17. Multiple regression for each metric without interaction terms on precip.	44
Table 18. Multiple regression for each metric and all 1, 2, 3, and 4-way interaction terms	45

ACKNOWLEDGEMENTS

I would like to offer a huge thanks to my mentor and guide, Dr. Ritzi, for his scholarly advice and help with my scientific approach, and for providing valuable feedback on the phrasing and organization of this manuscript. I would also like to thank Mike Bottomley from Wright States statistical consulting service for his insight and help with the statistical analysis. Lastly, I would like to thank the United States Historical Climate Network and the National Oceanic and Atmospheric Administration for making precipitation, temperature, and the indices representing the strength of each perturbations historical data records easily available to the public.

I. INTRODUCTION

Teleconnections are defined as links between large-scale ocean-atmospheric perturbations and globally distal weather (Wallace et al., 1981; Nigam et al., 2015). Large-scale ocean-atmospheric perturbations include the North Atlantic Oscillation (NAO), the El Niño Southern Oscillation (ENSO), the Pacific Decadal Oscillation (PDO), and the Atlantic Multidecadal Oscillation (AMO). Teleconnections have been identified between these ocean-atmospheric perturbations and resulting anomalies in distal weather across the continents (e.g., Ropelewski et al., 1987; 1989; Hurrell, 1995; Mantua et al., 1997; Enfield et al., 2001; Mantua et al., 2002; McCabe et al., 2004; Knight et al., 2006; Lindsey, 2016; 2017; and NOAA CPC, 2022). Examples of studies identifying teleconnection-caused weather anomalies in specific North American watersheds include Gabric et al. [date unknown], Mitra et al., 2014, and Ritzi et al., 2021.

Ritzi et al. (2021) examined historical records of winter precipitation and temperature in southwestern Ohio to determine if there were statistically significant differences due to teleconnections with ENSO. The data that were used were the measured monthly average of daytime high temperatures, and the monthly average of daily precipitation published by the U.S. Historical Climate Network (USHCN). The USHCN data were measured at station USH00338552 located near Urbana, OH (Figure 1). Their study used three statistical methods that included a regression analysis, where the ENSO cycle was represented by the extended Multivariate ENSO Index, MEI (NOAA). Winter was taken to be the 5 months from November to March, and three metrics were used in the analyses: the mean-monthly value, the maximum-monthly value, and the minimum-monthly value.

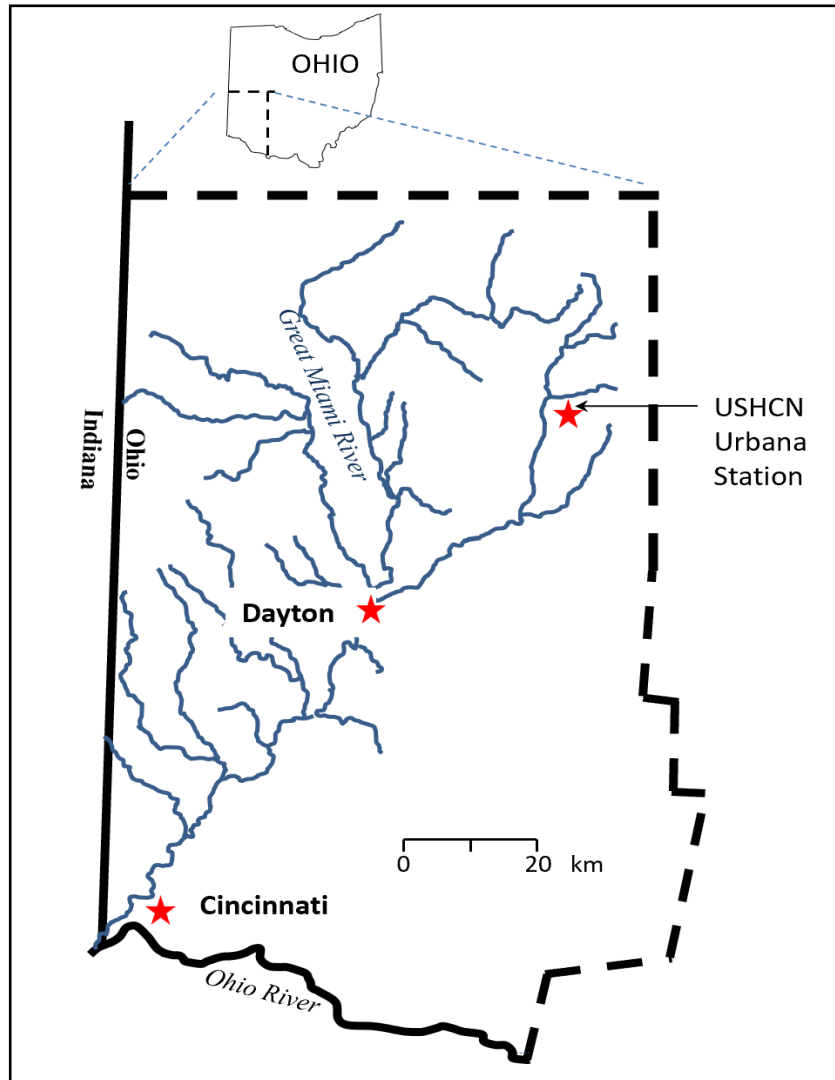


Figure 1. Southwest Ohio study area and data location. USHCN – U.S. Historical Climate Network. Modified from Ritzi et al. (2021)

The results showed that while most (80%) of El Niño winters had below average precipitation, and precipitation decreased with increasing MEI values, variations in MEI only accounted for 3% of the overall variability in precipitation. Furthermore, during La Nina winters precipitation was not statistically significantly different from neutral years. Temperature was also not found to be statistically significantly different than neutral years for either phase of ENSO.

The goal of this thesis is to expand on Ritzi et al. (2021) by considering and including, in addition to ENSO, three other large-scale perturbations in atmospheric circulation in the regression analysis. Each might have an individual teleconnection with winter temperatures in southwest Ohio and there might be combined effects. The three additional perturbations are the NAO, PDO, and AMO (Figure 2). While support for an ENSO effect was small for precipitation and nonexistent for temperature at the Urbana station (Ritzi et al., 2021), one of the additional perturbations newly considered here, and combinations of these perturbations including combinations with ENSO, might cause an identifiable and statistically significant anomaly in winter temperature or precipitation. The same historical data record of precipitation and temperature from USHCN will be used, but with additional data reflecting the strength of other perturbations in addition to the MEI data. The same statistical methods will be used to analyze each additional data record alone, and additional statistical methods, described below, will be used to analyze the combined records. The additional methods include multiple regressions with and without interaction terms.

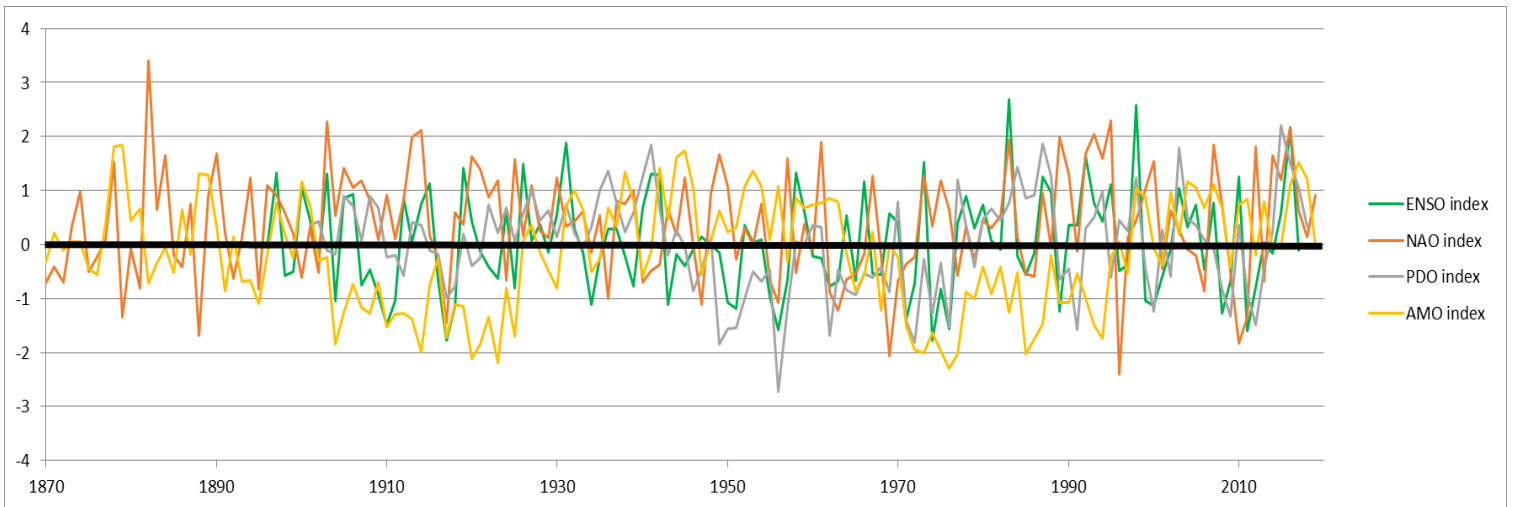


Figure 2. Indices representing four types of global perturbations. The El Niño Southern Oscillation (ENSO), the North Atlantic Oscillation (NAO), the Pacific Decadal Oscillation (PDO), and the Atlantic Multidecadal Oscillation (AMO).

The organization of the thesis is as follows. In Chapter 2, the northern hemisphere jet streams and Polar Vortex along with each perturbation's (ENSO, PDO, NAO, and AMO) effect on the jet streams are reviewed. Furthermore, existing knowledge of teleconnections with winter weather in southwest Ohio is reviewed. In Chapter 3 the data and methodologies used in this thesis are described. In Chapter 4 the results from the analysis for effects on winter temperature are presented, and in Chapter 5 the results from the analysis for effects on winter precipitation are presented. Chapter 6 contains a discussion of the results, and conclusions are drawn in Chapter 7.

II. BACKGROUND AND PREVIOUS WORK

II.A. Jet Streams and the Polar Vortex

The teleconnection between perturbations in atmospheric/ocean circulation patterns like ENSO and distal weather is facilitated in large part through alterations in the pattern of the jet streams (Woolings, 2022). Thus, it is helpful to first discuss relevant aspects of the jet streams. Jet streams are thin regions of high velocity air that move eastward around the globe near the tropopause level. In the northern hemisphere, there are two persistent meandering jet streams known as the subtropical (or Pacific) and the polar jet streams and a less persistent Arctic jet stream, that form near the three fold structure of the tropopause (dashed lines in Figure 3). Each jet stream can vary in location, but in general the subtropical jet stream is highest in elevation and located along the northern side of the hadley cell around 25° N and is driven by northward angular momentum transport in the hadley cell from the suns direct thermal influence (Held et al., 1980; Shapiro et al., 1986; Woolings, 2022). The polar jet stream is second in elevation and found above the polar front around 45° N, and it is driven by momentum and heat fluxes from eddies of the mid-latitudes located within the polar front (Williams, 1988; Shapiro et al., 1986; Panetta et al., 1988). The Arctic jet stream is the lowest in elevation, and located around 70° N (Shapiro et al., 1986), but its influence on the study area is not considered since it is not in close proximity to the Midwestern U.S. like the polar and subtropical jet streams.

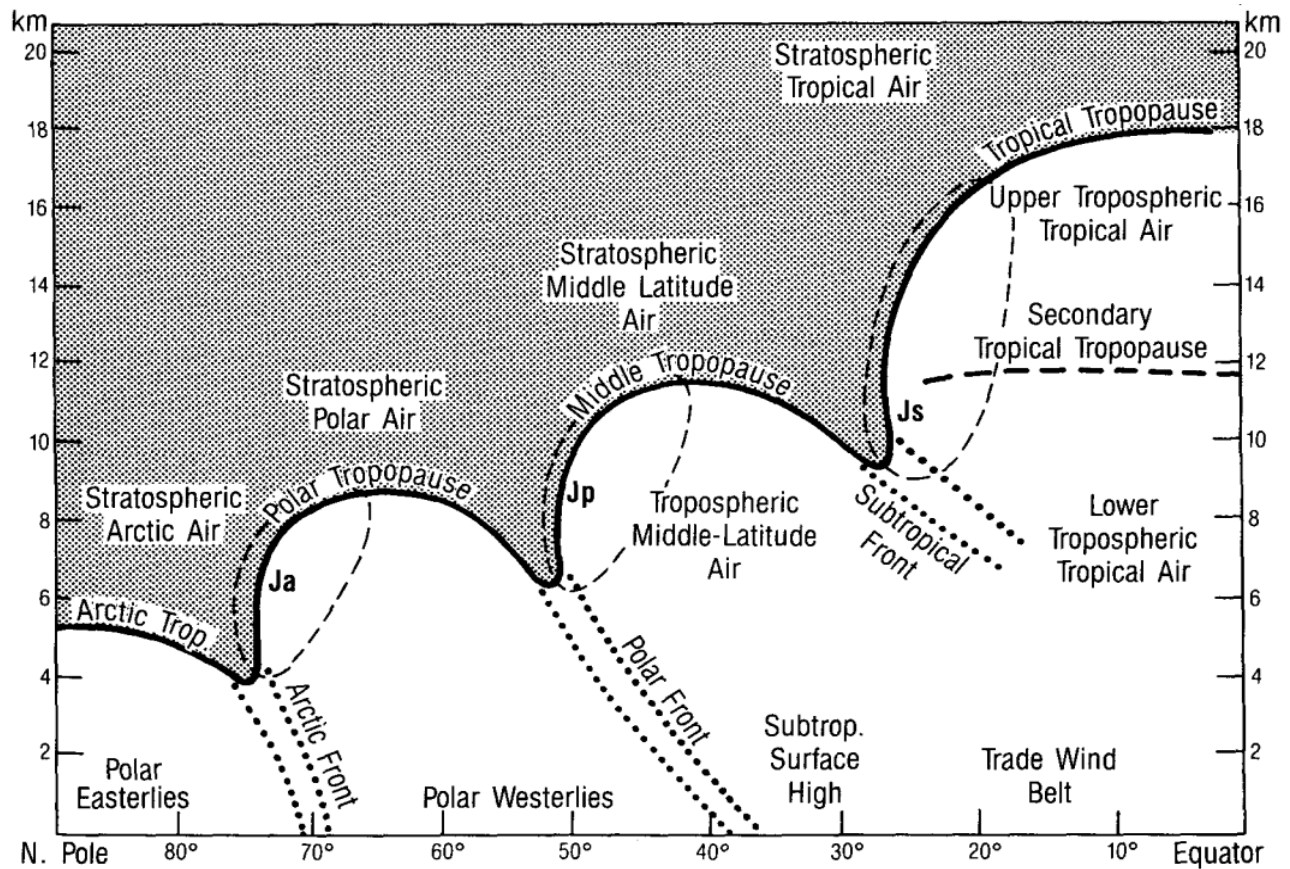


Figure 3. Idealized model of the threefold structure of the tropopause. Elevation is on the y-axis, while latitude is on the x-axis. The dark black line represents the tropopause between the stratosphere above (shaded) and the troposphere below (white). The thick dotted lines represent the primary frontal zones that extend through the depth of the troposphere, and the thin dashed lines encircle the cores of the three primary jet streams (Ja is the Arctic jet, Jp is the polar jet, and Js is the subtropical jet). From Shapiro et al., 1986.

The North Atlantic Oscillation, discussed further below, is related to the stability of the polar vortex, which in turn is related to the position of the polar jet stream. The polar jet stream and the polar vortex occur in separate layers of the atmosphere, however, they can affect each other. When the polar vortex, which occurs in the stratosphere, is strong and stable it has a stabilizing influence on the polar jet stream in the troposphere which confines cold air to the north pole region. But when the polar vortex is weak and unstable the polar jet stream can start to

wobble, allowing cold troughs of air to migrate south. Thus it is the polar jet stream that actually delivers cold air to mid latitudes when the polar vortex is disrupted. (Figure 4; Lindsey, 2021)

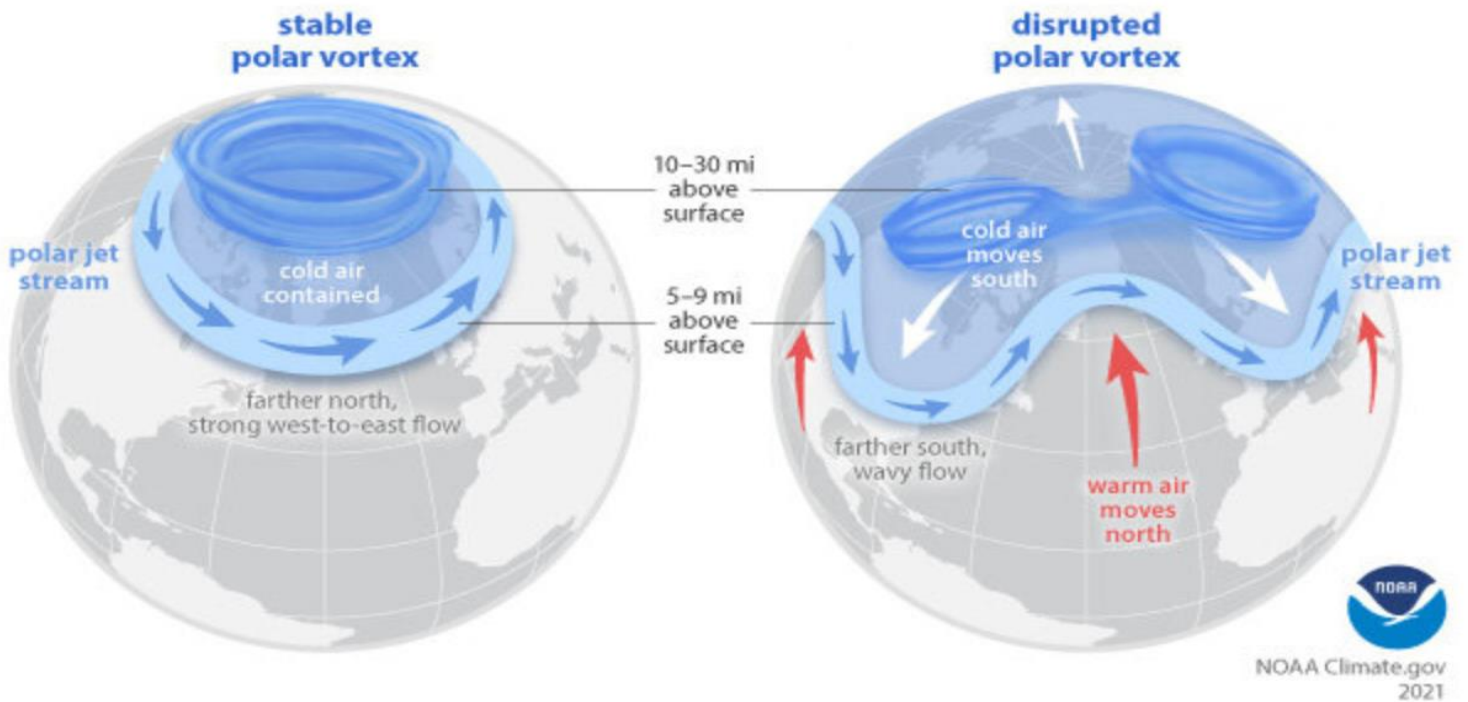


Figure 4. When the Arctic polar vortex is especially strong and stable (left globe), it encourages the polar jet stream, down in the troposphere, to shift northward. The coldest polar air stays in the Arctic. When the vortex weakens, shifts, or splits (right globe), the polar jet stream often becomes extremely wavy, allowing warm air to flood into the Arctic and polar air to sink down into the mid-latitudes. From Lindsey (2021).

The stratosphere and troposphere are best coupled in the winter, and thus jet stream variability in response to stratospheric perturbations is more pronounced in the winter (Hall et al., 2015). Among the winter jet stream variations, those of the subtropical and polar jet streams most affect the winter weather in temperate mid-latitudes, the region of focus in this study (Riehl, 1962; Hoskins et al., 1990).

Manney et al., (2014) showed the winter positions of the polar and subtropical jet streams, averaged from 1979 – 2012, are most often found around 58° N at an altitude of 8.9 km and around 29° N at an altitude of 11.5 km, respectively. Therefore, the Midwestern U.S. is typically located between the winter jet stream positions, with the polar jet stream to the north and the subtropical jet stream to the south. However, as discussed below, significant variations in the positions of these jet streams may be caused by perturbations in circulations patterns in the Atlantic region, including the North Atlantic Oscillation (NAO) and Atlantic Multidecadal Oscillation (AMO), and by perturbations arising in the Pacific region including the El Nino Southern Oscillation (ENSO) and the Pacific Decadal Oscillation (PDO). Significant variations in jet stream positions in response to these global circulation phenomena can cause local weather variability referred to as anomalies, which are defined in this study as a clear difference between the weather during an event like an ENSO phase, and the normal conditions that are averaged over many years. Anomalies in temperature and precipitation, as well as other attributes of weather, occur across the United States. The goal of this thesis is to identify anomalies that may exist in winter temperature and precipitation in southwest Ohio as caused by teleconnections with NAO, AMO, ENSO, and PDO individually or as combined influences.

In the next sections, perturbations in global ocean and atmospheric circulation that affect the jet streams are reviewed individually.

II.B. El Nino Southern Oscillation (ENSO)

The ENSO is a perturbation in ocean-atmospheric circulation that originates in the Pacific with major centers occurring in either the central or eastern tropics (Capotondi et al., 2015, Lindsey, 2017, Yang et al., 2018, Feng et al, 2019). ENSO is marked by the oscillation between El Nino (warm) and La Nina (cold) phases that involves changes in sea surface temperature

(SST), air temperature, wind circulation and other ocean-atmospheric properties. This alternating pattern of warm and cold sea surface anomalies in the tropical Pacific has been shown to oscillate on interannual timescales with periods lasting 2-7 years (Ropelewski et al., 1987, Garrison, 2010). Many indices have been used to measure the strength of perturbations in global ocean and atmospheric circulation in relation to ENSO, but the extended Multivariate ENSO Index (MEI) is used in this study because it is available for the century-long time of recorded data for temperature and precipitation records. The extended MEI is determined from sea level pressure, zonal and meridional components of the surface wind, sea surface temperature, surface air temperature and cloudiness using data from the International Comprehensive Ocean-Atmosphere Data Set (Wolter, 2011; 2018). The MEI is increasingly positive with the strength of the El Niño phase and increasingly negative with the strength of the La Niña phase.

Under normal conditions (neutral phase), air and surface water flow westward across the Pacific, leading to the upwelling of cold water along the west coast of South America (Figure 5). However, During El Niño events the trade winds that usually blow westward diminish and reverse, leading to an eastward movement of warm water that is backed up against the west coast of South America as a warm zone (Figure 5a; Garrison, 2010). The warming of the tropical troposphere, strengthens the Hadley cell circulation, displacing the subtropical jet stream farther north than normal (Lindsey, 2017; Yang et al., 2018). During La Niña events the conditions representing normal become more extreme, with stronger westward currents, and powerful upwelling along the coast of South America, leading to a cold zone forming (Figure 5b; Garrison, 2010). The colder tropical troposphere air then weakens the Hadley cell circulation, and the unstable polar jet stream can migrate southward (Lindsey, 2017).

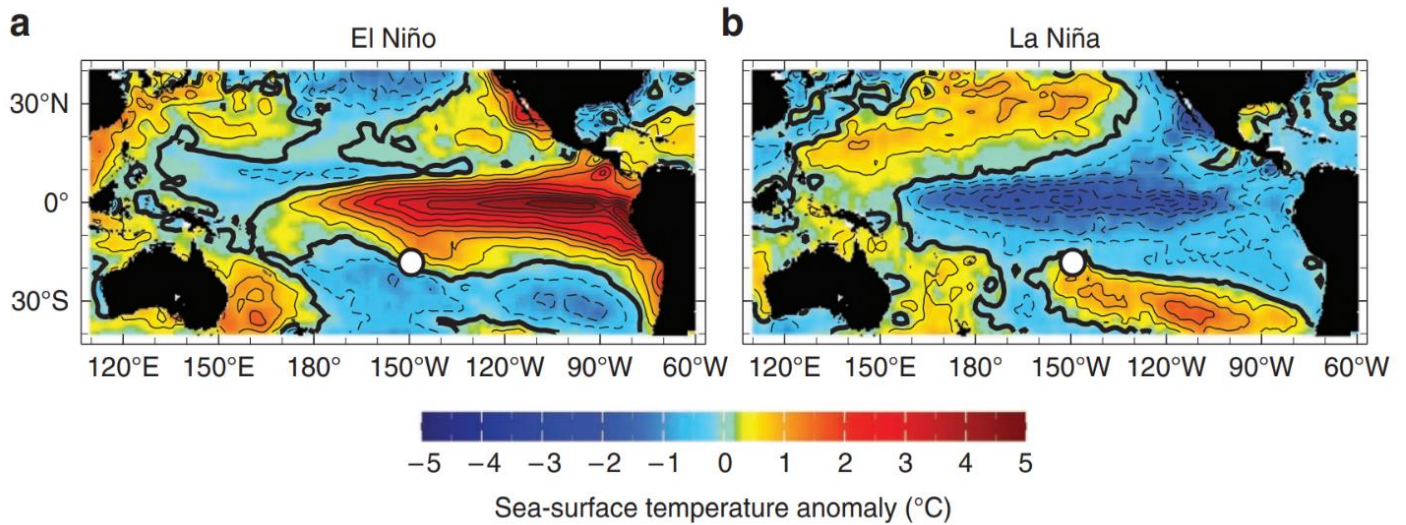


Figure 5. Composite maps of sea-surface temperature anomalies for moderate to strong (a) El Niño and (b) La Niña events during the period 1982–2008 (November–February). The location of Tahiti (and Integrated Ocean Drilling Program site M0024) in the tropical South Pacific is indicated by the white dot (not investigated in this study). From Felis et al., 2012

The jet streams then transmit these ENSO effects into the midlatitudes, and continental scale studies have suggested that in the Midwestern United States the winter precipitation and temperature are affected by the phase of ENSO. During La Niña conditions the polar jet stream dips below the Midwest which can bring colder temperatures with more precipitation to the midwest, while the opposite occurs to the southeast. During El Niño conditions the subtropical Jet Stream can extend across the United States in a position beneath the midwest which can bring higher temperatures and less precipitation to the midwest, while bringing the cold and more precipitation to the southeast (Figure 6; Trenberth et al., 1998; Garrison, 2010; Lindsey, 2017).

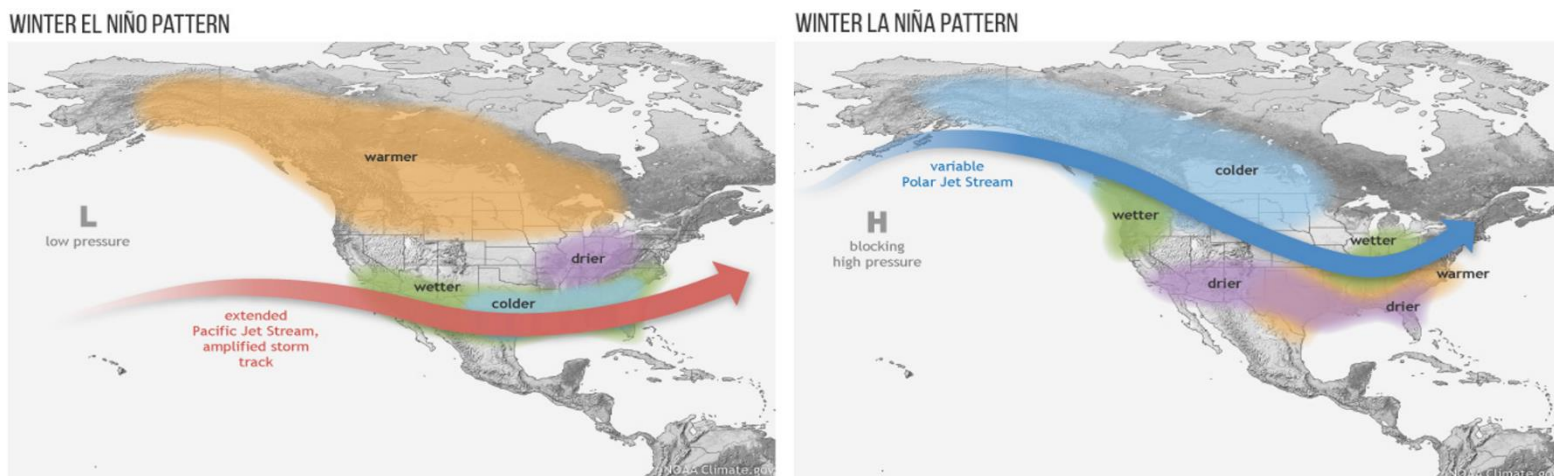


Figure 6. The expected temperature and precipitation effects related to jet stream position during El Niño (left image) and La Niña (right image). From Lindsey (2017).

In contrast to continental studies, Ritzi et al. (2021) analyzed a record of winter temperature and precipitation for 121 winters, from 1896 to 2016, for statistically significant anomalies corresponding to El Niño and La Niña conditions in southwest Ohio (figure 1). Their research hypothesis, built from these continental scale studies, was that El Niño winters have been warmer with less precipitation and La Niña winters have been colder with more precipitation.

The data used were the measured monthly average of daytime high temperatures, and the monthly average of daily precipitation published by the U.S. Historical Climate Network (USHCN). The USHCN data were measured at station USH00338552 located near Urbana, OH (Figure 1). The ENSO cycle was represented by the extended Multivariate ENSO Index, MEI (NOAA). The results from their study (Table 1, Figure 7) showed that (1) eighty percent of El Niño winters had below average precipitation, with an average anomaly of -5 cm, (2) the MEI regressed against precipitation showed a statistically significant negative slope, but the variance in MEI only explained 3% of the overall variability in winter precipitation, (3) La Niña winters were not statistically significantly different from neutral year winters, and (4) winter temperature

was not statistically significantly different during El Niño or La Niña winters within the century of record.

Table 1. Results from linear regression for USHCN data.
Modified from Ritzi et al. (2021)

Winter Temperature (°C)			
	Slope	p-value	Adj. R ²
Mean Monthly	-6.5E-05	0.9996	<1E-9
Maximum-Month	-0.07855	0.6994	<1E-3
Minimum-Month	-0.05143	0.8286	<1E-4
Winter Precipitation (cm)			
	Slope	p-value	Adj. R ²
Mean Monthly	-0.38823	0.0257	0.0331
Maximum-Month	-0.06129	0.0550	0.0224
Minimum-Month	-0.18779	0.2205	0.0043

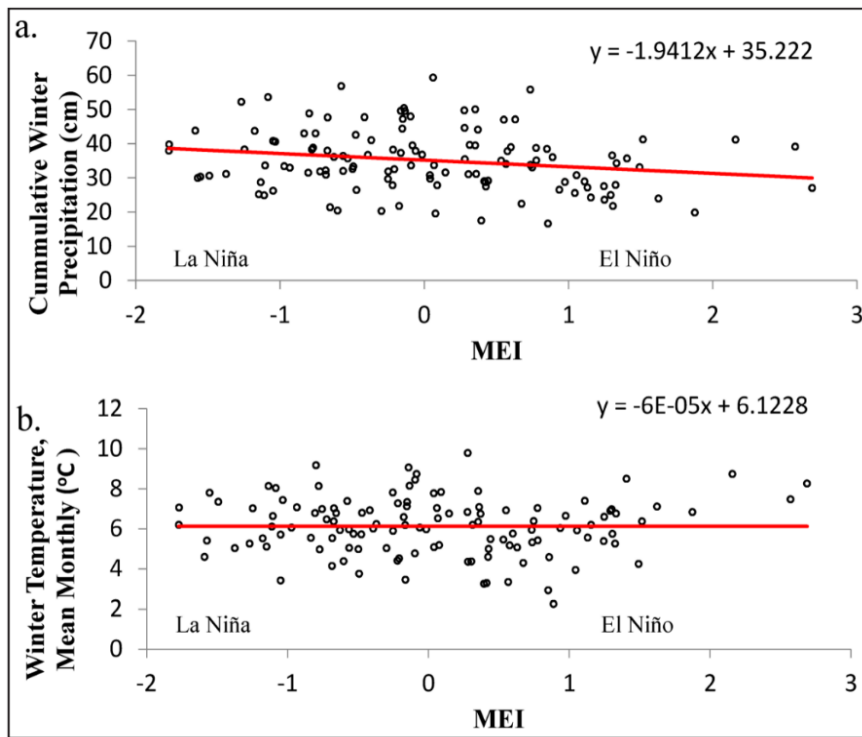


Figure 7. Examples of linear regression for (a) cumulative winter precipitation and (b) mean monthly winter temperature (daily highs) vs. the extended Multivariate ENSO Index (MEI). From Ritzi et al. (2021).

II.C. Pacific Decadal Oscillation (PDO)

The PDO is a perturbation in ocean-atmospheric circulation that also originates in the Pacific, but with its major signatures in the northern extratropics (above 20° N) and a less prominent secondary signature located in the tropics that coincides with the major signature displayed during ENSO events (Mantua et al., 2002). The perturbation is marked as either being in a warm phase where there is a cold center in the Northern Pacific with a boomerang shaped warm anomaly along the west coast of North America, or as being in a cold phase that has the reverse pattern, with a warm center in the Northern Pacific and a cold anomaly along the coast of North America (Mantua, 2002; Liberto, 2016). Figure 8 shows the different sea surface temperature patterns observed during different phases of the PDO, and their relationship to phases of ENSO. This oscillation from warm to cold phases related to PDO happens on decadal timescales with periods lasting 20 – 30 years (Mantua et al., 1997; 2002).

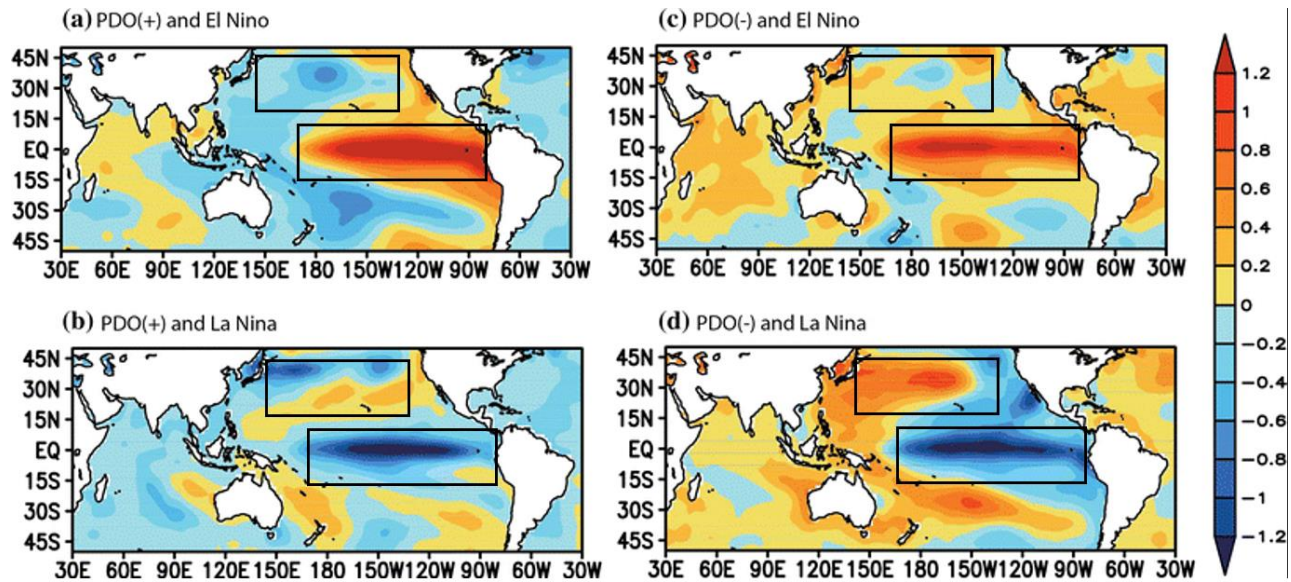


Figure 8. Composite map of sea surface temperature (°C) during (a) warm phase of the Pacific Decadal Oscillation (PDO) and El Niño years, (b) the warm phase of the PDO and La Niña years, (c) the cold phase of the PDO and El Niño years, (d) the cold phase of the PDO and La Niña years. Upper boxes show dominant PDO signature, and lower box shows dominant El Niño Southern Oscillation signature. Modified from Zhao et al., 2016

PDO results from a complex combination of processes that span the tropical and extratropical latitudes. These processes can include anything from fluctuations in the Aleutian low, teleconnections from the tropics through the atmospheric bridge, or midlatitude ocean dynamics like reemergence and gyre circulation (Trenberth, 1998; Liberto, 2016, Newman et al. 2016). The PDO index, which measures the strength of the perturbation, is based on NOAA's extended reconstruction of sea-surface temperatures (SSTs). When SSTs are anomalously cool in the interior North Pacific and warm along the western Pacific Coast, the PDO has a positive value, but when the anomaly patterns are reversed with warm SST in the interior and cool sea-surface temperature anomalies along the North American coast, the PDO has a negative value (Mantua et al., 1997; 2002).

With PDO being remotely forced in part from teleconnections with the tropics, PDO is intricately linked to low-frequency modulations of ENSO. Furthermore, since the two perturbations have similar patterns of Pacific Ocean-atmospheric warming, but ENSO oscillates on shorter timescales, PDO is often viewed as a long-lived El Niño like pattern of Pacific variability (Zhang et al., 1997; Mantua et al., 1997). The similar patterns of ocean-atmospheric warming as compared to ENSO, means the PDO alone likely has comparable shifts in the jet streams as well. Figure 9 shows how correlations with precipitation and temperature across the U.S. can be similar for ENSO and PDO. However, anomalies in SST can become different during periods when PDO and ENSO are in phase as compared to when they are out of phase (Figure 8), which may create different anomalies in winter weather. For example, when El Niño winters occur during positive PDO phases (in phase), the Atlantic SST can be colder than usual (Figure 8a), but when they are out of phase the Atlantic SST can be warmer than usual (Figure 8c). Conversely, when La Niña winters occur during negative PDO phases (in phase), the

Atlantic SST can be warmer than usual (Figure 8d), but when they are out of phase the Atlantic SST can be colder than usual (Figure 8c). This relationship with the Atlantic SST may alter the phase of perturbations that originate in the Atlantic, and lead to interaction effects that contribute to different temperature and precipitation anomalies as compared to when the perturbations are working alone.

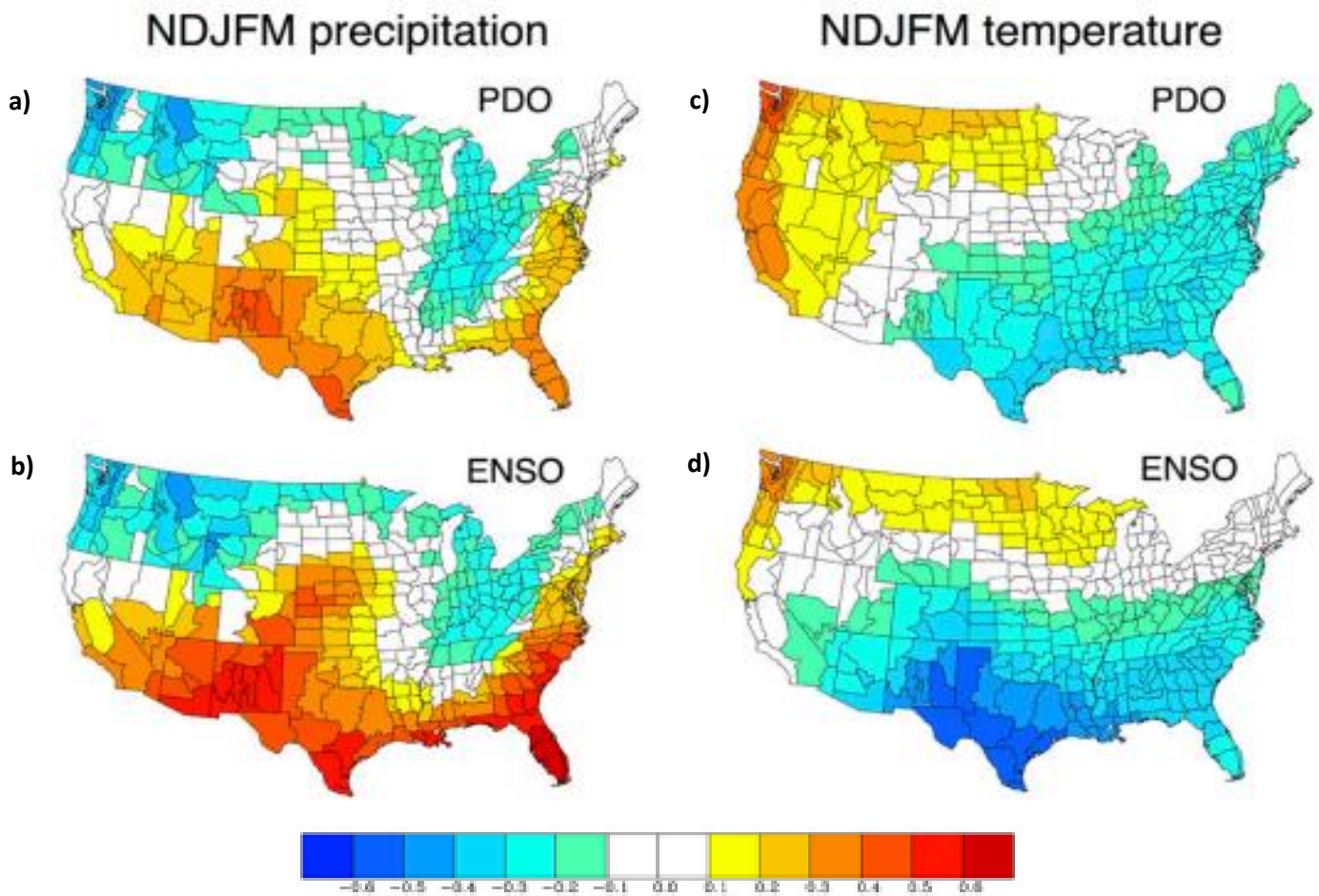


Figure 9. Cold season relationship between the Pacific Decadal Oscillation (PDO), and the El Niño Southern Oscillation (ENSO), and U.S. precipitation and temperature anomalies determined from U.S. climate division data (Vose et al. 2014), for the years 1901–2014. NDJFM U.S. precipitation anomalies correlated with (a) the PDO index, and (b) the ENSO index. NDJFM U.S. temperature anomalies correlated with (c) the PDO index, and (d) the ENSO index. Modified from Newman et al., 2016.

II.D. North Atlantic Oscillation (NAO)

The NAO, first identified by Walker and Bliss (1932), is a large ocean-atmospheric phenomenon located in the North Atlantic Ocean that is said to dominate winter weather variability over the north Atlantic and surrounding lands (Hurrell et al., 1995). Often considered as a regional expression of the Arctic oscillation that is specific to the north Atlantic, the NAO is also seen as a surface expression of the polar vortex (Kennedy et al., 2014). When the NAO is in a strong phase, the subtropical high-pressure system near the Azores and the subpolar low-pressure system near Iceland are more pronounced, and the larger pressure gradient between them pulls stronger westerly winds across the Atlantic that helps to strengthen and stabilize the polar vortex. Conversely, when the NAO is in a weak phase, the subtropical high and the subpolar low are less pronounced with weakened westerlies across the Atlantic and a disrupted polar vortex (Hurrell, 1995; Lindsey et al., 2009; NOAA, 2012, Kennedy et al., 2014, Lindsey, 2021). Figure 10 shows the 700 millibar (mb) geopotential heights (pressure) anomalies associated with the strong and weak phases of the NAO. This oscillation between large and small pressure differentials from the Azores high and the Icelandic low has been shown to occur on decadal timescales (Hurrell, 1995), although, the typical cycle of NAO is about 2 weeks (Feldstein, 2000; 2003).

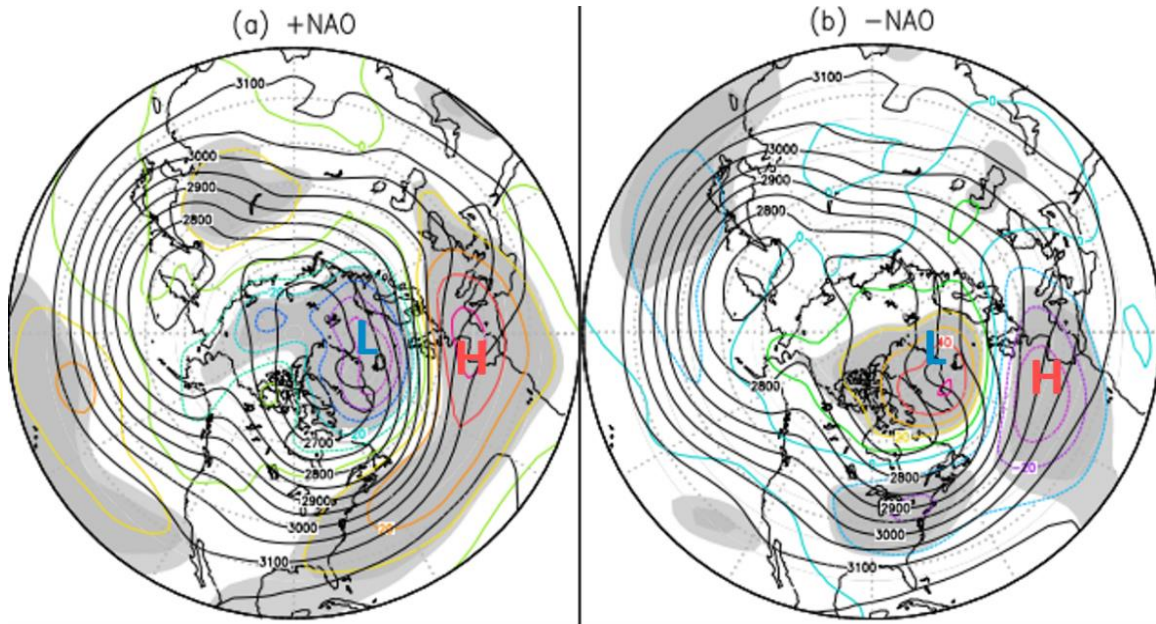


Figure 10. Composite maps of mean winter 700 millibar (mb) geopotential height (in black solid lines) and anomalies (in color) (relative to NAO-neutral mean) for winters of (a) strong and (b) weak NAO during 1963–2010. The interval for the means and anomalies is 50 and 10 m, respectively. The low pressure near Iceland is shown with a blue L, and the high pressure over the Azores is shown with a red H. The gray and dark shaded areas represent the 95% and 99% significance level, respectively. Modified from Bai et al., 2012.

The NAO index is based on the surface sea-level pressure difference between the Subtropical High near Azores and the Subpolar Low near Iceland, where the differing strengths between the two causes the pressure gradient between them to oscillate, controlling how strong the winds are that move across the Atlantic (Hurrell, 1995). When the sea level pressure distribution over the north Atlantic has a well-developed subpolar low and Azores high, the larger pressure gradient between them gives a positive NAO index, which is associated with stronger westerly winds across the Atlantic that keep cold and possibly wet air from migrating into the midlatitudes. Conversely, when the subpolar low and Azores high are rather weak, the smaller pressure gradient between them gives rise to a negative NAO index, thus reducing the westerlies strength across the Atlantic and allowing cold and possibly wet air to migrate into the Midlatitudes (Figure 11; Wanner et al. 2001; Booth et al., 2006; Lindsey et al., 2009, NOAA, 2012). Most

studies of the effects the NAO has on hydrologic factors have focused on Europe, and the eastern United States, but Balvanz et al. (2017) found that NAO does affect snowfall in the Midwestern United States. In fact, all eleven stations studied had a negative correlation between the NAO index and snowfall, suggesting snowfall in the Midwest is more likely and potentially heavier when the NAO index is negative.

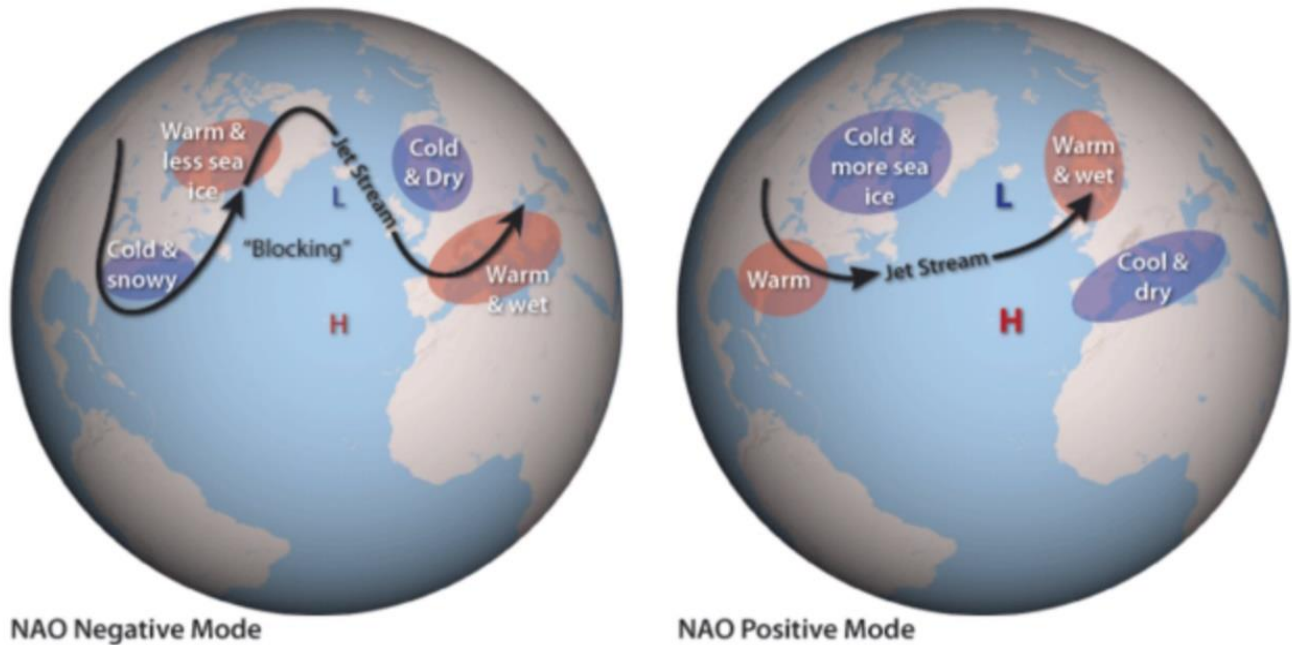


Figure 11. Expected temperature and precipitation effects along with jet stream positions related to the phases of NAO. From Lindsey et al. (2009), which was adapted from the AIRMAP by Ned Gardiner and David Herring, NOAA.

II.E. Atlantic Multidecadal Oscillation (AMO)

The AMO is another ocean-atmospheric perturbation originating from the Atlantic that has been identified as an important mode of weather variability. AMO describes the alteration between warm and cold SST anomalies in the North Atlantic with a 40 to 80-year cycle (Kerr, 2000; Enfield et al., 2001; Knight et al., 2006). Typically, the SST changes by about 1 °C between warm and cold phases (Enfield et al., 2001). Figure 12 shows an example of a warm phase AMO pattern averaged from 1951 to 1980.

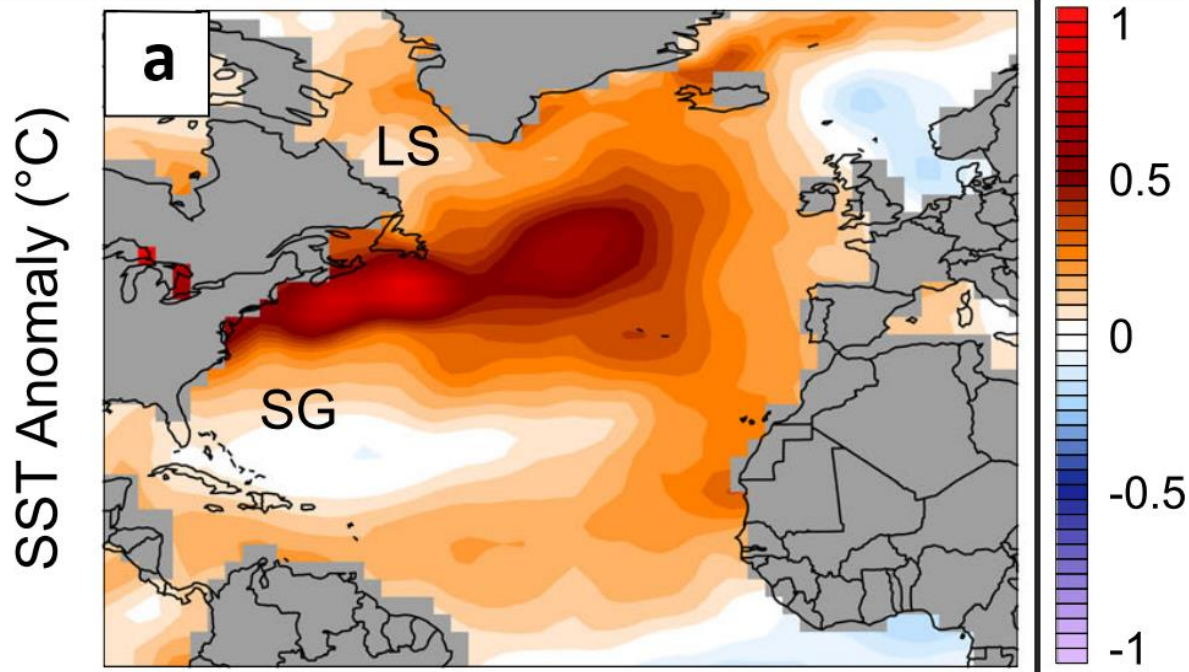


Figure 12. Mean SST anomaly map (1951–1980) for warm AMO years (Positive Phase). The Labrador Sea (LS) and Sargasso Sea (SG) are labeled for reference. Modified from Birkel, 2018.

The AMO index is calculated by linearly detrending and applying a running 10-year mean to the monthly SST anomalies and then averaging the values over the North Atlantic (0° - 70° N, 80° W- 10° E; Enfield et al, 2001). The index becomes increasingly positive as the North Atlantic becomes increasingly warmer and is increasingly negative as the North Atlantic becomes increasingly colder.

During a negative AMO index, global circulation patterns favor above average precipitation across much of the U.S., which includes the Midwest (Enfield et al., 2001). Conversely, during a positive AMO index, circulation patterns cause drier conditions across much of the U.S. and the Midwest (McCabe et al., 2004). Winter temperature anomalies related to AMO do not seem to be directly investigated in the literature, possibly because of the lack of interchange between positive and negative phases warrants poor statistical analyses, but recent studies relating the phase of AMO to the phase of NAO present an indirect influence through

modulation of the polar jet stream (Davini et al., 2015; Kwon et al., 2020). These studies show that a positive AMO phase can ultimately lead to a negative NAO response and a southward displaced polar jet stream. Conversely, a negative AMO phase can lead to a positive NAO response and a poleward displaced polar jet stream. As shown by NAO above, this suggests that a positive AMO phase may create colder conditions in the Midwest, and that a negative AMO phase may create warmer conditions in the Midwest.

II.F. Interactions between ENSO, PDO, NAO, and AMO

Exploring interactions between each of the four ocean-atmospheric perturbations and the respective global circulation patterns could explain more of the variance in hydrologic attributes than explained by any single perturbation alone. For example, Enfield et al. (2001) shows AMO has a strong influence on summer rainfall over the contiguous U.S. and may modulate the strength of the teleconnection between ENSO and winter precipitation. Furthermore, Zhang et al. (2007) suggested AMO might serve as one of the sources or triggers of North Pacific multidecadal variability like PDO, and McCabe et al. (2004) attributed more than 50% of the U.S. spatial and temporal variance in multidecadal drought frequency to the PDO and AMO. More recently, Johnson et al. (2020) showed that even though tropical Pacific weather variability is the primary driver for PDO, it is also modulated by multi-basin interactions originating from the Atlantic and, together, the tropical Pacific and the Atlantic basins explain roughly 52-73% of the PDO variability. Also, Børgel et al. (2020) found the AMO influences the east-west position of the Icelandic Low and the Azores High, with a NW to SE shift during positive AMO phases, and in return this could affect how the NAO interacts with distal weather.

In summary, the literature suggests that the four phenomena and their interactions have a combined effect on US weather. Therefore, our general hypothesis is that statistically significant anomalies in Southwestern Ohio winter weather have occurred from teleconnections with large-

scale ocean-atmospheric perturbations including ENSO, PDO, NAO, and AMO. In table 2, the hypotheses to be tested here for winter weather anomalies in the historical record caused by perturbations in addition to ENSO are listed and are depicted for temperature in Figure 13. Another hypothesis to be tested here is that when combinations of these perturbations exist, larger anomalies have occurred in the historical record creating more variance in the overall record as compared to anomalies from any individual perturbation alone.

Table 2. Hypotheses for each individual perturbations effect on winter temperature and precipitation in Southwest Ohio.

Record	Positive Conditions				Negative Conditions			
Temperature (°C)	<u>ENSO</u> Warmer	<u>PDO</u> Warmer	<u>NAO</u> Warmer	<u>AMO</u> Colder	<u>ENSO</u> Colder	<u>PDO</u> Colder	<u>NAO</u> Colder	<u>AMO</u> Warmer
Precipitation (cm)	Drier	Drier	Drier	Drier	Wetter	Wetter	Wetter	Wetter

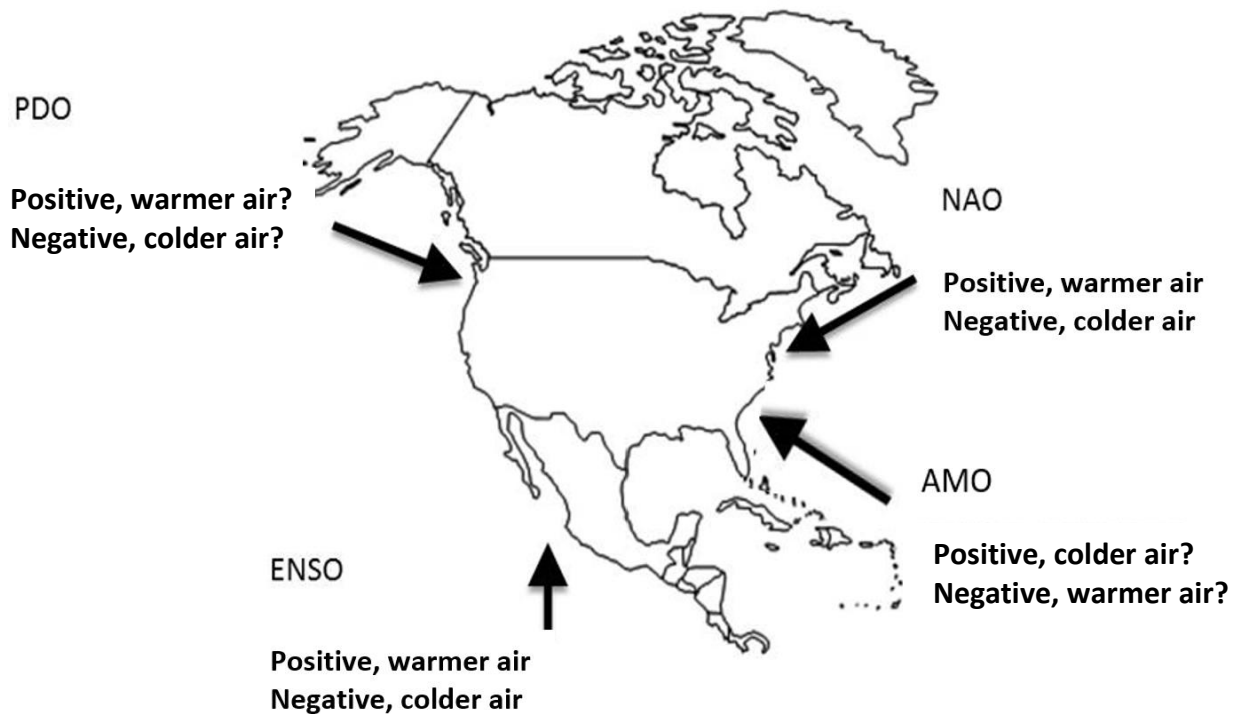


Figure 13. Expected temperature affects for each positive and negative phase index based on continental scale studies

III. DATA AND METHODS

III.A. Data

The sample population of data for winter precipitation and temperature used by Ritzi et al. (2021) are again used here and are from the US National Historical Climate Network (USHCN; NOAA NCEI [see distribution websites listed in the references below as USHCN; NOAA NCEI date unknown a, unknown b]). Specifically, the data are the monthly average of daytime high temperatures and the monthly average precipitation, both measured at station USH00338552, near Urbana, OH (Latitude = 40.1, Longitude = -83.7833; Figure 1) and consists of 121 winters from 1896 to 2016. The indices reflecting the strength of the ENSO, PDO, NAO and AMO perturbations are from the National Oceanic and Atmospheric Administration (NOAA) Climate Prediction Center (CPC). The ENSO cycle is represented by the extended multivariate ENSO Index, MEI (Wolter, 2011; 2018). The NAO cycle is represented by the NAO Index, NAO hereafter (Hurrell, 1995; NOAA PSL, 2013). The PDO cycle is represented by the PDO Index, PDO hereafter (Mantua et al., 1997; Zhang et al., 1997; NOAA PSL, 2018). The AMO cycle is represented by the AMO Index, AMO hereafter (Enfield et al., 2001, NOAA PSL, date unknown). Time series for each of these indices are shown in Figure 2.

We use three metrics for temperature and precipitation: the mean-monthly winter value (i.e., winter 5-month mean), which might show seasonal-scale anomalies, and the maximum-month value (i.e., the value for the month with the highest value within each winter) and the minimum-month value which both might show a shorter one-month scale anomaly as compared to the winter mean. Summary statistics for temperature and precipitation for each of these metrics are shown in Table 3, and time series of cumulative precipitation and average temperature are shown in Figure 14.

Table 3. Summary statistics for metrics on winter temperature and precipitation for each perturbation

Winter Temperature (°C)						
	All winters		Positive winters		Negative winters	
	<u>Mean</u>	<u>Std. Dev.</u>	<u>Mean</u>	<u>Std. Dev.</u>	<u>Mean</u>	<u>Std. Dev.</u>
NAO						
Mean-monthly	6.12	1.43	6.42	1.49	5.59	1.16
Maximum-month	11.68	2.06	11.82	2.11	11.41	1.97
Minimum-month	1.10	2.41	1.57	2.48	0.25	2.04
PDO						
Mean-monthly	6.12	1.45	5.91	1.49	6.36	1.38
Maximum-month	11.69	2.09	11.25	1.88	12.19	2.21
Minimum-month	1.05	2.43	0.88	2.43	1.24	2.45
AMO						
Mean-monthly	6.12	1.43	6.35	1.42	5.97	1.43
Maximum-month	11.68	2.06	11.58	2.09	11.74	2.06
Minimum-month	1.10	2.41	1.86	2.29	0.59	2.37
Winter Precipitation (cm)						
	All winters		Positive winters		Negative winters	
	<u>Mean</u>	<u>Std. Dev.</u>	<u>Mean</u>	<u>Std. Dev.</u>	<u>Mean</u>	<u>Std. Dev.</u>
NAO						
Mean-monthly	7.03	1.78	7.28	1.81	6.58	1.65
Maximum-month	122.14	46.44	125.84	46.53	115.42	46.05
Minimum-month	32.02	15.60	33.56	16.51	29.22	13.52
PDO						
Mean-monthly	7.00	1.77	6.76	1.93	7.28	1.54
Maximum-month	121.84	46.56	120.33	51.28	123.56	40.89
Minimum-month	31.88	15.81	29.61	14.46	34.49	16.99
AMO						
Mean-monthly	7.03	1.78	7.37	1.76	6.80	1.77
Maximum-month	122.14	46.44	128.65	53.47	117.70	40.78
Minimum-month	32.02	15.60	32.67	15.24	31.58	15.93

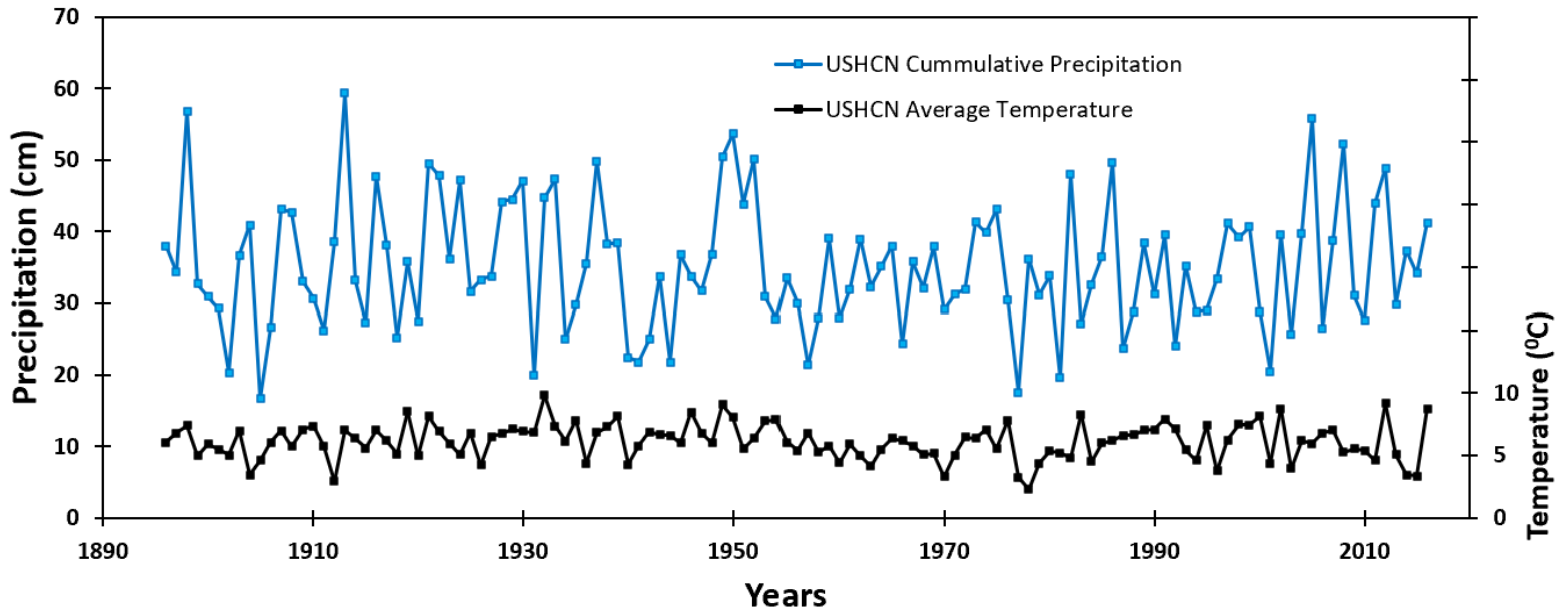


Figure 14. Records for winter weather. Cumulative precipitation is for November through March. Temperature is the average daily high in winter. USHCN – U.S. Historical Climate Network.

III.B. Methods

To test the hypotheses for temperature and precipitation anomalies presented in table 2, the statistical analyses are broken up into two parts: (1) anomalies caused by perturbations individually, and (2) anomalies caused by the combined influence of perturbations.

III.B.1. Testing hypotheses for anomalies caused by perturbations individually

Three statistical methods are used. The first two methods separate the data into positive and negative phases for each index, and the third method uses the entire continuous cycle. The first method was to quantify the proportion of positive phase winters for which a metric fell above and below the century long mean (CLM), and the proportion of negative phase winters for which it fell above/below the CLM. The second method was to use an independent samples t-test comparison of the mean value of a metric for positive phase winters against the mean of negative phase winters to test whether the means are statistically significantly different. The third method was to consider the effect from the entire continuous cycle of each perturbation by analyzing the variations in temperature and precipitation metrics as a function of the respective index, using

linear regression. Assumptions of constant variance and normality of error terms were tested by visual inspection of residual plots and were satisfied for all metrics of each added index.

III.B.1.A. Proportion of positive phase winters with temperature or precipitation above or below negative phase winters

As stated above, the first method was to simply quantify the proportion of positive phase winters for which a metric fell above and below the century long mean (CLM), and the proportion of negative phase winters for which it fell above/below the CLM. To illustrate, a result supportive of the positive PDO hypotheses would be that the sample proportion of positive phase winters had an average temperature greater than that of the CLM, and that the entire 95% confidence interval falls above 0.5. Confidence intervals are calculated using the Wilson score interval methodology (Wilson, 1927).

III.B.1.B. Independent sample t-tests comparison of the mean winter values between positive and negative phase indices

Statistical tests for differences in the means are constructed with a null hypothesis (H_0) that is hoped to be rejected. Therefore, the H_0 is that the mean during positive phase winters is equal to the mean during negative phase winters, and rejection of the H_0 is defined in this study as a probability of error that is less than 0.05 for one-tailed tests (Kutner et al., 2013). When the H_0 is rejected, the alternate hypothesis (H_A) is supported. For example, in considering the average temperature in positive PDO phase winters, the H_A states that the mean was higher than for negative PDO phase winters.

III.B.1.C. Simple Linear Regression

An example of a result consistent with the research hypothesis would be a regression model for average temperature vs. PDO that is statistically significant ($p\text{-value} \leq 0.05$) and has a negative slope. Further, An R^2 value above 0.25 indicates the PDO explains a meaningful proportion of the variation in temperature (Cohen, 1988), while a value below 0.25 would not

support this conclusion. Similar examples drawn from the hypotheses in Table 2 could be given for the other indices as well.

III.B.2. Testing hypotheses for anomalies cause by the combined influence of perturbations

MEI was included as an independent variable in multiple regression with NAO, PDO, and AMO. A multiple regression without considering terms for interactions between the indices was first conducted, followed by a multiple regression that includes terms for interactions between the four indices. Here, the variance inflation factor (VIF) for all four predictor terms is checked and found to be well below the value of 5 that would begin to raise concern for multicollinearity (Kutner et al., 2013).

III.B.2.A. Multiple Linear Regression without interactions

A first order “main effects” multiple regression model incorporating ENSO, NAO, PDO, and AMO without considering the interaction effects is used first. The main effects model gives the additive effect of the four indices together and is given by the general formula in equation 1.

$$\hat{Y} = \hat{\beta}_0 + \hat{\beta}_1 X_1 + \hat{\beta}_2 X_2 + \hat{\beta}_3 X_3 + \hat{\beta}_4 X_4 \quad \text{(Eq.1)}$$

Where, \hat{Y} is the estimated response variable for the chosen hydrologic attribute, X_1 is MEI, X_2 is NAO, X_3 is PDO, X_4 is AMO, β_0 is the y-intercept, and β_k is the slope for a given X_k .

A result consistent with the general hypotheses here would be a model with statistically significant predictor variables, and a larger R^2 value than found in any of the linear regressions, indicating that adding more terms to the regression analysis increases the amount of variance explained. Furthermore, an R^2 value above 0.25 would indicate the model explains a meaningful proportion of the variance in temperature or precipitation.

III.B.2.B. Multiple Linear Regression with interactions

A first order multiple regression model that incorporates the four indices as well as all 2, 3 and 4-way interactions between them is used, and Equation 2 shows the general formula for the model when all combinations of interactions are accounted for.

$$\begin{aligned}\hat{Y} = & \widehat{\beta}_0 + \widehat{\beta}_1 X_1 + \widehat{\beta}_2 X_2 + \widehat{\beta}_3 X_3 + \widehat{\beta}_4 X_4 + \widehat{\beta}_5 X_1 X_2 + \widehat{\beta}_6 X_1 X_3 + \widehat{\beta}_7 X_1 X_4 \\ & + \widehat{\beta}_8 X_2 X_3 + \widehat{\beta}_9 X_2 X_4 + \widehat{\beta}_{10} X_3 X_4 + \widehat{\beta}_{11} X_1 X_2 X_3 + \widehat{\beta}_{12} X_1 X_2 X_4 \\ & + \widehat{\beta}_{13} X_1 X_3 X_4 + \widehat{\beta}_{14} X_2 X_3 X_4 + \widehat{\beta}_{15} X_1 X_2 X_3 X_4\end{aligned}\quad \text{(Eq.2)}$$

Where, \hat{Y} is the estimated response variable for the chosen hydrologic attribute, X_1 is MEI, X_2 is NAO, X_3 is PDO, X_4 is AMO, β_0 is the y-intercept, and β_k is the slope for a given predictor term.

A result consistent with the hypotheses here would be at least one statistically significant (p-value ≤ 0.05) interaction term and an R^2_a value that is above that found in the additive model, indicating some interactions between these perturbations are important in explaining the variance in temperature or precipitation.

IV. RESULTS FOR TEMPERATRE

Presented here are the results of sample proportions, and differences in the means, followed by the regression analyses of temperature, for each metric. The analysis of sample proportions above or below the mean for each phase of the index and the analysis of differences in the means among each positive and negative phase index are presented together first. Then, the regression analyses are presented sequentially, first with an analysis of temperature vs. each index individually, then vs. the four indices together in one multiple-regression, and finally with a multiple regression that includes terms for interactions between the indices.

IV.A. Analysis of sample proportions and differences in means among each positive and negative phases

The sample proportions of positive phase winters above the century long mean (CLM) and negative phase winters below the CLM for each metric and index are shown in Table 4, along with the 95% CI. Of positive NAO winters, 62% of them had above average temperatures in the minimum-month with its 95% CI entirely above 0.5, and 60% of winters had mean monthly temperature greater than the CLM with a CI that is close to but not entirely above 0.5 (0.49 to 0.71). Of negative NAO winters, 67% of them had mean monthly temperature below the CLM, and 70% had below average temperatures in the minimum-month of a winter, and both have the 95% CI entirely above 0.5. These results support the hypotheses that positive NAO winters are associated with above average temperatures, and negative NAO winters are associated with below average temperatures. For PDO and AMO the proportions for all metrics and their 95% CI are not entirely above/below 0.5 as per the hypotheses in Table 2, and therefore the results do not support those hypotheses.

Table 4. Results for the sample proportions of positive and negative phase indices according to the hypotheses from Table 2

Winter Temperature (°C) ^a		
	Proportion of positive phases above mean (CI)	Proportion of negative phases below mean (CI)
NAO (n = 121)		
Mean Monthly	0.60 (0.49, 0.71)	0.67 (0.53, 0.81)
Maximum-Month	0.49 (0.38, 0.60)	0.58 (0.43, 0.73)
Minimum-Month	0.62 (0.51, 0.72)	0.70 (0.56, 0.83)
PDO (n = 116)		
Mean Monthly	0.47 (0.34, 0.59)	0.44 (0.31, 0.58)
Maximum-Month	0.42 (0.30, 0.54)	0.50 (0.37, 0.63)
Minimum-Month	0.53 (0.41, 0.66)	0.48 (0.35, 0.61)
	Proportion of positive phases below mean (CI)	Proportion of negative phases above mean (CI)
AMO (n = 121)		
Mean Monthly	0.49 (0.35, 0.63)	0.50 (0.38, 0.62)
Maximum-Month	0.55 (0.41, 0.69)	0.47 (0.36, 0.59)
Minimum-Month	0.45 (0.31, 0.59)	0.47 (0.36, 0.59)

^a Highlighted values color key: Green, proportion and 95% confidence interval (CI) all above 50%. Yellow, proportion above 50% but not the 95% CI. Red, proportion not above 50%.

The results for statistical tests of the difference in the means between positive and negative phase winters for each temperature metric are shown in Table 5. The mean monthly temperature during positive NAO winters was on average 0.82 °C higher than that of winters with a negative NAO index, and the minimum month metric was 1.32 °C more. These differences are statistically significant with p -values of 0.0005 and 0.0011, respectively. This result supports the hypotheses that positive NAO winters are warmer than negative NAO winters.

The differences for the mean monthly and maximum month temperature metrics between positive and negative PDO phases were statistically significant ($p=0.0477$, $p=0.0084$), but were negative, counter to the hypothesis that positive phase PDO winters were warmer than winters in the negative PDO phase.

For AMO, the minimum month metric was found to be statistically significant with positive phase winters being on average 1.27 °C warmer than negative phase winters. This result is counter to the hypothesis that positive-phase AMO winters are colder than winters with AMO in the negative phase.

Table 5. Results for the differences in the means among positive and negative phase indices.

Winter Temperature					
	Difference (°C)	H₀^a	H_A^b	Result^c	p-value
NAO+ VS NAO-					
Mean-Monthly	0.82	Equal Means	> Mean	Reject H ₀	0.0005
Maximum-Month	0.42	Equal Means	> Mean	Fail to Reject H ₀	0.1413
Minimum-Month	1.32	Equal Means	> Mean	Reject H ₀	0.0011
PDO+ VS PDO-					
Mean-Monthly	-0.45	Equal Means	> Mean	Fail to Reject H ₀	0.0477
Maximum-Month	-0.94	Equal Means	> Mean	Fail to Reject H ₀	0.0084
Minimum-Month	-0.36	Equal Means	> Mean	Fail to Reject H ₀	0.2122
AMO+ VS AMO-					
Mean-Monthly	0.38	Equal Means	< Mean	Fail to Reject H ₀	0.0738
Maximum-Month	-0.17	Equal Means	< Mean	Fail to Reject H ₀	0.3340
Minimum-Month	1.27	Equal Means	< Mean	Reject H ₀	0.0019

^a H₀ is the null hypothesis in hopes to reject

^b H_A is the alternate hypothesis extracted from Table 2

^c Highlighted values color key: Green, reject the null hypothesis with p-value less than 0.05. Yellow, cannot reject the null hypothesis at the 0.05 level but p-value is close. Red, cannot reject the null hypothesis.

Collectively, these results give an indication that there is a teleconnection between NAO oscillations and winter temperature in the study area, and do not support the hypotheses for teleconnections between the PDO and AMO and winter temperature in the study area.

IV.B. Separate regression on each index

The results of regression on each index individually against each metric are given in Table 6 and Figure 15. The slope for the regression model “NAO” is positive with p -values well below 0.05, consistent with the hypothesis that winters are increasingly warmer when NAO is increasingly positive and increasingly colder when NAO is increasingly negative. The R^2 value is 0.14 indicating that NAO alone does not account for much of the variance in winter temperature, however it is much higher than the R^2 value for the models using other indices including ENSO (Tables 1 and 6). The results for the other indices and other metrics have either an inconsistent slope, p -value above 0.05, or a negligible R^2 value, and do not support the respective hypothesis for an individual effect associated with those perturbations.

Table 6. Temperature regression, results with each individual index on each metric

Winter Temperature ($^{\circ}$C) ^a			
	Coefficients	p-value	R^2
NAO (n = 121)			
Mean Monthly	0.5464	2.6E-05	0.139
Maximum-Month	0.3837	0.046	0.033
Minimum-Month	0.5137	0.022	0.043
PDO (n = 116)			
Mean Monthly	-0.3616	0.016	0.050
Maximum-Month	-0.3357	0.124	0.021
Minimum-Month	-0.5172	0.041	0.036
AMO (n = 121)			
Mean Monthly	0.2226	0.070	0.026
Maximum-Month	-0.0039	0.983	4E-6
Minimum-Month	0.5319	0.012	0.052

^a Highlighted values color key: Green, slope is consistent with hypotheses or p -value is less than 0.05. Yellow, p -value is close to 0.05 but slightly above. Red, slope is inconsistent with hypotheses or p -value is greater than 0.05 or adjusted R^2 value is less than 0.25.

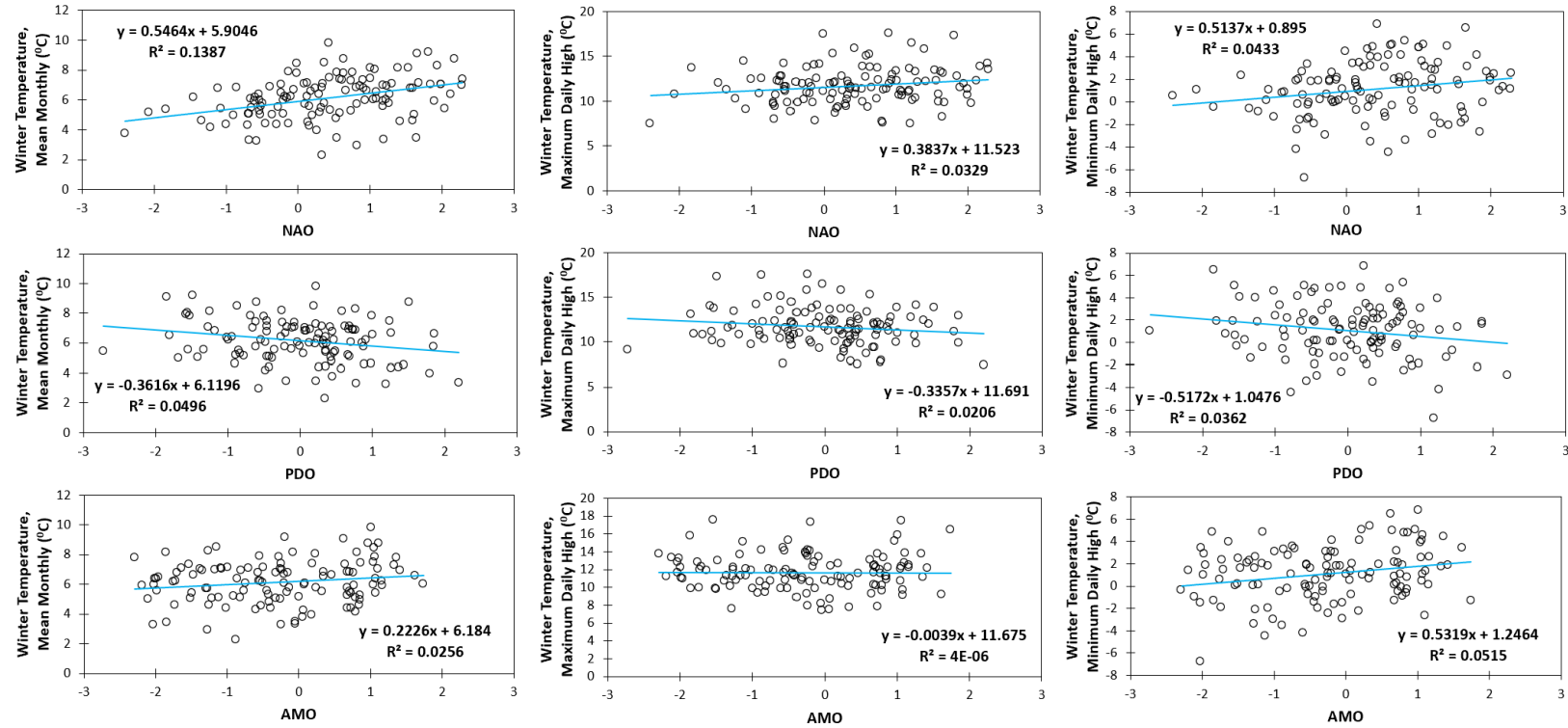


Figure 15. Linear regressions for each index individually (NAO in the first row, PDO in the second row, and AMO in the third row) against each of the metrics chosen (mean-monthly winter temperatures in first column, Maximum-month temperature in the second column, Minimum-month temperature in the third column).

IV.C. Multiple regression with four indices

The results of the multiple regression analysis on temperature using the indices MEI, NAO, PDO and AMO are given in Table 7. The R^2 for the mean monthly winter temperature model was 0.14 with NAO alone but increases to an adjusted R^2 (R^2_a) of 0.23 when all four indices are included in the regression. For the minimum-month metric it increases from 0.04 to 0.13. Thus, more variance in the metrics is explained in the multi-variate model. However, the NAO index has the smallest p-value among all three metrics and is the most significant.

Table 7. Multiple regression for each metric without considering interaction terms (n=116).

Winter Temperature (°C) ^a						
Terms	Mean Monthly		Maximum Month		Minimum Month	
	<u>coefficient</u>	<u>p-value</u>	<u>coefficient</u>	<u>p-value</u>	<u>coefficient</u>	<u>p-value</u>
Intercept	5.963	< 2E-16	11.54	< 2E-16	0.965	6.7E-05
MEI	0.070	0.6509	0.012	0.961	0.047	0.864
NAO	0.629	1.83E-06	0.429	0.036	0.671	0.003
PDO	-0.443	0.0057	-0.377	0.140	-0.579	0.041
AMO	1.808	0.0094	0.291	0.793	3.437	0.005
R^2_a	0.23		0.027		0.125	
p -value	1.2E-06		0.136		0.0008	

^a Highlighted values color key: Green, p-value is less than 0.05 or R^2_a is greater than or equal to 0.25. Yellow, p-value is close to 0.05 but slightly above or R^2 is close to 0.25. Red, p-value is greater than 0.05 or adjusted R^2 value is much less than 0.25.

IV.D. Multiple regression with four indices and interactions

In further analysis, the interactions between variables were added as interaction terms in the various combinations of independent variable groupings. Because the four-way interaction term was insignificant (p-value > 0.05) it was removed and the multiple regression was re-run without it, with results shown in Table 8. Beyond individual terms, only the three-way interaction term that includes NAO with MEI and PDO was significant (p-value = 0.043). The adjusted R^2 for the mean-monthly metric model increased from 0.23 (without interactions) to 0.25 (with interactions) and, therefore, we focus on the three-way interaction model for the mean-monthly metric.

Table 8. Multiple regression for each metric with All 1, 2, and 3-way interaction terms (n=116)

Winter Temperature (°C) ^a						
Terms	Mean Monthly		Maximum Month		Minimum Month	
	<u>coefficient</u>	<u>p-value</u>	<u>coefficient</u>	<u>p-value</u>	<u>coefficient</u>	<u>p-value</u>
Intercept	5.937	< 2E-16	11.60	< 2E-16	0.900	0.001
MEI	0.063	0.7336	0.161	0.597	-0.098	0.769
NAO	0.538	0.0003	0.394	0.105	0.548	0.040
PDO	-0.510	0.0046	-0.466	0.113	-0.576	0.074
AMO	2.014	0.0181	0.117	0.933	5.273	0.0008
MEI: NAO	0.082	0.6006	-0.111	0.670	0.107	0.706
MEI: PDO	-0.036	0.8172	-0.210	0.416	0.037	0.897
MEI: AMO	2.165	0.0491	2.335	0.198	2.400	0.226
NAO: PDO	-0.156	0.3499	-0.199	0.471	-0.136	0.652
NAO: AMO	0.228	0.7671	0.622	0.625	-1.627	0.244
PDO: AMO	-0.926	0.3681	-1.138	0.504	-0.277	0.882
MEI: NAO: PDO	0.274	0.0431	0.228	0.305	0.165	0.497
MEI: NAO: AMO	-0.968	0.3050	-1.264	0.418	-1.634	0.339
NAO: PDO: AMO	0.057	0.9598	1.508	0.420	-2.226	0.278
R^2_a	0.25		0.0075		0.12	
p-value	3.5E-05		0.396		0.013	

^a Highlighted values color key: Green, p-value is less than 0.05 or R^2_a is greater than or equal to 0.25. Yellow, p-value is close to 0.05 but slightly above or R^2 is close to 0.25. Red, p-value is greater than 0.05 or adjusted R^2 value is much less than 0.25. Gray, regression term is already being expressed in the highest order interaction terms and is not considered as supporting or rejecting the hypothesis here.

The plot of interactions in the model between MEI, NAO, and PDO in Figure 16 shows that the trend in the interactions is towards the warmest winters occurring when NAO is positive while MEI and PDO are negative, and towards the coldest winters occurring when NAO is negative while MEI and PDO are positive.

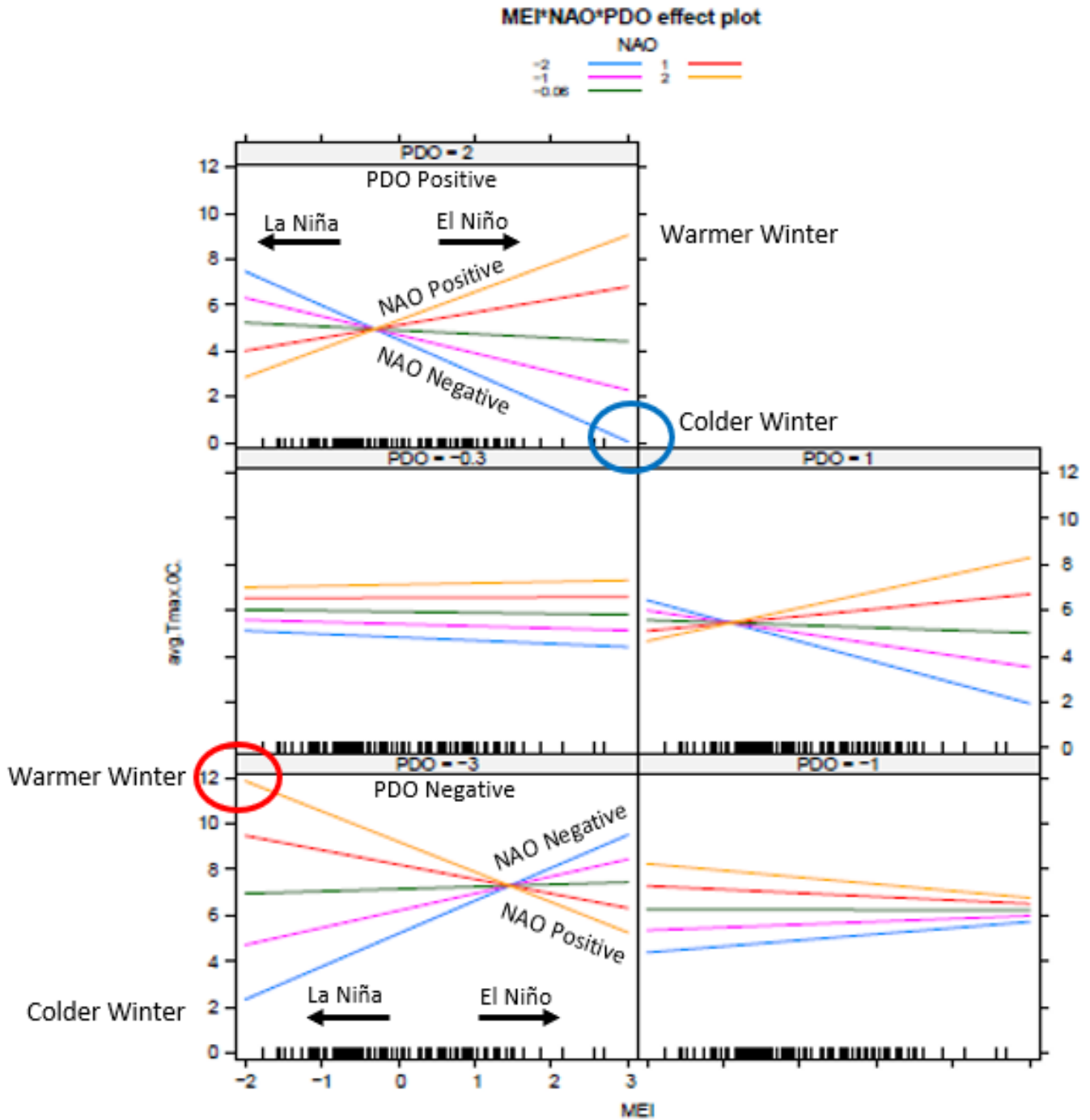


Figure 16. Three-way interaction model for the mean monthly temperature ($^{\circ}\text{C}$) metric. The model gives the warmest winter temperature prediction when NAO is positive and MEI and PDO are negative (red circle) and gives the coldest winter temperature prediction when NAO is negative and MEI and PDO are positive (blue circle).

These observed trends in the interactions hint at an NAO influence on winter temperature that is more pronounced under the conditions when the NAO index is opposite the PDO and MEI. These two conditions represent 2 of 8 possible combinations of the positive/negative phases among these indices, as shown in Table 9 and 10. Combination 4 is when NAO is negative and MEI and PDO are positive and is indicated to be associated with colder winter temperature, while Combination 6 is when NAO is positive and MEI and PDO are negative and is indicated to be associated with warmer winter temperature (Table 10).

Table 9. Eight combinations of index states (positive, negative) for NAO, PDO, and MEI.

Terms	Combinations							
	1	2	3	4	5	6	7	8
NAO	Positive	Positive	Negative	Negative	Positive	Positive	Negative	Negative
MEI	Positive	Positive	Positive	Positive	Negative	Negative	Negative	Negative
PDO	Positive	Negative	Negative	Positive	Positive	Negative	Negative	Positive

Table 10. Statistics for monthly winter temperature for years under each combination of perturbations given in table 9 and for all years.

Interactions	Mean Monthly Winter Temp. (°C)	Standard Dev.	Observations
Combination 1	6.17	1.76	25
Combination 2	6.21	1.38	11
Combination 3	6.09	1.29	8
Combination 4	5.20 (coldest)	1.20	12
Combination 5	6.31	1.21	17
Combination 6	6.93 (warmest)	1.46	21
Combination 7	5.77	1.10	14
Combination 8	5.33	1.08	8
All years	6.12	1.43	116

This led to proceeding with a more refined research hypothesis that winters under combination 4 were colder than average and winters under combination 6 were warmer than average. The temperatures for these combinations are plotted in comparison with the mean for all years in Figure 17. 83% of winters under combination 4 fell below the mean and 71% of winters under combination 6 fell above the mean, with the entire 95% confidence interval above 50% for both (Table 11). These results support the refined hypotheses that winters tend to be colder under the conditions represented by combination 4 and warmer under the conditions of combination 6.

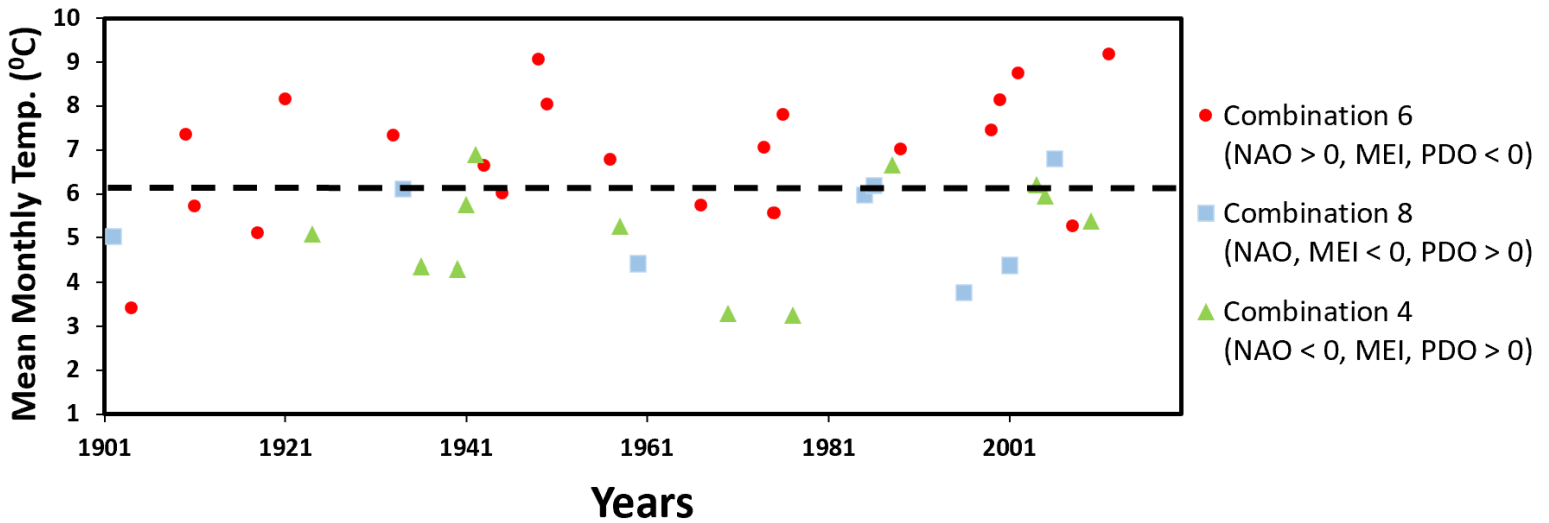


Figure 17. mean monthly temperature at the Urbana station from 1901 to 2016 for combinations 4, 6, and 8. The black dashed line represents the mean winter temperature for all years on record and is 6.12 °C.

T-tests, assuming unequal variance, were used to compare the means of the different combinations given in table 6 to the means of years outside the combination to search for statistically significant differences between the means (Table 12). In Combinations 4, 6, and 8 the null hypothesis is rejected, and the data supports statistically significantly lower temperatures during combinations 4, and 8, while supporting statistically significantly higher temperatures during combination 6. This led to adding combination 8 to Figure 17.

Table 11. Proportion of combination 4, combination 6 and combination 8 winters with mean above/below the winter mean for other years (116 winters total, 12 as combination 4, 21 as combination 6, and 8 as combination 8).

Winter Temperature ^a			
	Proportion of Combination 4 below mean for all other years	Proportion of Combination 6 above mean for all other years	Proportion of Combination 8 below mean for all other years
Mean-Monthly	0.83 (0.62, 0.99)	0.71 (0.52, 0.91)	0.75 (0.50, 0.99)
Maximum Month	0.42 (0.14, 0.70)	0.57 (0.36, 0.78)	0.75 (0.45, 0.99)
Minimum Month	0.74 (0.51, 0.99)	0.67 (0.47, 0.87)	0.88 (0.65, 0.99)

^a Highlighted values color key: Green, proportion and 95% confidence interval (CI) all above 50%. Yellow, proportion above 50% but not the 95% CI. Red, proportion not above 50%.

Table 12. Results from hypothesis testing on differences in the mean with unknown and unequal variances.

Winter Temperature					
	Anomaly (°C)	H ₀ ^a	H _A ^b	Result ^c	p-value
Combination 4					
Mean-Monthly	-1.03	Equals Mean	< Mean	Reject H ₀	0.008
Maximum-Month	-0.22	Equals Mean	< Mean	Fail to Reject H ₀	0.357
Minimum-Month	-1.95	Equals Mean	< Mean	Reject H ₀	0.016
Combination 6					
Mean-Monthly	0.99	Equals Mean	> Mean	Reject H ₀	0.004
Maximum-Month	1.28	Equals Mean	> Mean	Reject H ₀	0.021
Minimum-Month	1.22	Equals Mean	> Mean	Reject H ₀	0.037
Combination 8					
Mean-Monthly	-0.85	Equals Mean	< Mean	Reject H ₀	0.034
Maximum-Month	-1.55	Equals Mean	< Mean	Reject H ₀	0.036
Minimum-Month	-1.07	Equals Mean	< Mean	Reject H ₀	0.032

^a H₀ is the null hypothesis in hopes to reject

^b H_A is the alternate hypothesis drawn from Figure 17

^c Highlighted values color key: Green, reject the null hypothesis with p-value less than 0.05. Yellow, cannot reject the null hypothesis at the 0.05 level but p-value is close. Red, cannot reject the null hypothesis.

In the analysis of variance (ANOVA), the overall F-test rejects the null hypothesis that all group means are equal (p -value = 0.03), which indicates at least one pair of combinations has statistically significantly different means. A multiple comparison procedure, using the Tukey-Kramer method (Haynes, 2013), at the 95% significance level is then used as a follow up test to look for where the specific differences between these groups of combinations occur (Table 13). The results show only the 6-4 combination has a p -value less than 0.05, indicating a statistically significant difference

between the mean winter temperature with winters under combination 6 being on average 1.7 °C warmer than winters under combination 4. This result is consistent with the hypothesis that the NAO is associated with more pronounced winter temperature anomalies when the NAO index is opposite the PDO, and MEI like that found in combinations 6 and 4.

Table 13. Multiple comparison between combinations

Winter Temperature ^a		
Pairwise Comparisons	Difference (°C)	p-value
Combinations 2 – 1	0.043	0.99
Combinations 3 – 1	-0.077	0.99
Combinations 4 – 1	-0.969	0.51
Combinations 5 – 1	0.141	0.99
Combinations 6 – 1	0.764	0.59
Combinations 7 – 1	-0.393	0.99
Combinations 8 – 1	-0.836	0.82
Combinations 3 – 2	-0.120	0.99
Combinations 4 – 2	-1.011	0.67
Combinations 5 – 2	0.098	0.99
Combinations 6 – 2	0.721	0.86
Combinations 7 – 2	-0.436	0.99
Combinations 8 – 2	-0.879	0.88
Combinations 4 – 3	-0.891	0.86
Combinations 5 – 3	0.218	0.99
Combinations 6 – 3	0.841	0.83
Combinations 7 – 3	-0.315	0.99
Combinations 8 – 3	-0.758	0.96
Combinations 5 – 4	1.109	0.42
Combinations 6 – 4	1.732	0.02
Combinations 7 – 4	0.576	0.97
Combinations 8 – 4	0.133	0.99
Combinations 6 – 5	0.623	0.87
Combinations 7 – 5	-0.534	0.96
Combinations 8 – 5	-0.976	0.73
Combinations 7 – 6	-1.157	0.25
Combinations 8 – 6	-1.600	0.12
Combinations 8 – 7	-0.443	0.99

^a Highlighted values color key: Green, reject the null hypothesis with p-value less than 0.05. Yellow, cannot reject the null hypothesis at the 0.05 level, but p-value is close. Red, cannot reject the null hypothesis.

V. RESULTS FOR PRECIPITATION

V.A. Analysis of sample proportions and differences in means among each positive and negative phases

The sample proportions of positive phase and negative phase winters above or below the CLM, corresponding to the hypotheses listed in Table 2 are shown in Table 14, along with the 95% CI. Of positive PDO winters, 74% have mean-monthly precipitation that is less than the CLM, and 68% have less precipitation during the maximum month of winter. These both have their 95% CI above 0.5, supporting the hypotheses that positive PDO winters are associated with below average precipitation. Also, 63% of positive AMO winters have less precipitation during the maximum month of winter. As for other metrics and indices, the 95% CI is not entirely above 0.5 as per the hypothesis in Table 2, and therefore the results do not support those hypotheses.

Table 14. Results for the sample proportions of positive and negative phase indices according to the hypotheses in Table 2

Winter Precipitation (cm)^a		
	Proportion of positive phases below mean (CI)	Proportion of negative phases above mean (CI)
NAO (n = 121)		
Mean Monthly	0.46 (0.35, 0.57)	0.33 (0.19, 0.47)
Maximum-Month	0.59 (0.48, 0.70)	0.21 (0.09, 0.33)
Minimum-Month	0.50 (0.39, 0.61)	0.47 (0.32, 0.61)
AMO (n = 121)		
Mean Monthly	0.47 (0.33, 0.61)	0.42 (0.30, 0.53)
Maximum-Month	0.63 (0.50, 0.77)	0.32 (0.21, 0.43)
Minimum-Month	0.49 (0.35, 0.63)	0.47 (0.36, 0.59)
PDO (n = 116)		
Mean Monthly	0.74 (0.63, 0.85)	0.37 (0.24, 0.50)
Maximum-Month	0.68 (0.56, 0.79)	0.35 (0.22, 0.48)
Minimum-Month	0.58 (0.46, 0.70)	0.56 (0.42, 0.69)

^a Highlighted values color key: Green, proportion and 95% confidence interval (CI) all above 50%. Yellow, proportion above 50% but not the 95% CI. Red, proportion not above 50%.

The results for statistical tests of the difference in the means between positive and negative phase winters for each precipitation metric are shown in Table 15. They indicate that positive NAO winters have on average 0.70 cm more precipitation than negative NAO winters with a p -value of 0.017, and positive AMO winters have on average 0.57 cm more precipitation than negative AMO winters with a p -value of 0.043. However, the means for positive phase NAO and AMO are above the means for negative phases, opposite to the hypotheses in Table 2, and therefore do not support those hypotheses. As for the PDO index, the difference in the means is consistent with the hypotheses in Table 2, with positive PDO winters having 0.53 cm less precipitation than negative PDO winters. The phases of PDO are not statistically significantly different from each other under the 95% significance level, although they are very close for the mean-monthly and minimum-month metrics ($p = 0.053$, and $p = 0.0506$, respectively).

Table 15. Results of t -tests for the differences in the mean among positive and negative phase indices

Winter Precipitation (cm)					
	Difference (cm)	H₀^a	H_A^b	Result^c	p-value
NAO+ VS NAO-					
Mean-Monthly	0.70	Equal Means	< Mean	Reject H ₀	0.0174
Maximum-Month	10.42	Equal Means	< Mean	Fail to Reject H ₀	0.1192
Minimum-Month	4.34	Equal Means	< Mean	Fail to Reject H ₀	0.0610
PDO+ VS PDO-					
Mean-Monthly	-0.53	Equal Means	< Mean	Fail to Reject H ₀	0.0528
Maximum-Month	-3.22	Equal Means	< Mean	Fail to Reject H ₀	0.3538
Minimum-Month	-4.88	Equal Means	< Mean	Fail to Reject H ₀	0.0506
AMO+ VS AMO-					
Mean-Monthly	0.57	Equal Means	< Mean	Reject H ₀	0.0425
Maximum-Month	10.95	Equal Means	< Mean	Fail to Reject H ₀	0.1142
Minimum-Month	1.08	Equal Means	< Mean	Fail to Reject H ₀	0.3530

^a H₀ is the null hypothesis in hopes to reject

^b H_A is the alternate hypothesis extracted from Table 2

^c Highlighted values color key: Green, reject the null hypothesis with p -value less than 0.05. Yellow, cannot reject the null hypothesis at the 0.05 level, but p -value is close. Red, cannot reject the null hypothesis.

Collectively, these results give an indication that there is a weak teleconnection between PDO oscillations and winter precipitation in the study area, and do not support the hypotheses for teleconnections between NAO and AMO and winter precipitation in the study area

V.B. Separate regression on each index

Results of regression on each index individually against each metric are given in Table 16 and Figure 18. The slope for the regression model of PDO is negative with a p -value below 0.05, consistent with the hypothesis that winters are increasingly drier when PDO is increasingly positive, and increasingly wetter when PDO is increasingly negative. However, the R^2 value is only 0.04 indicating little of the variance in precipitation is explained by PDO alone. The results for the other indices and other metrics have either an inconsistent slope, p -values above 0.05, or a negligible R^2 value and do not support the respective hypotheses for an individual effect associated with those perturbations.

Table 16. Precipitation regression, results on each individual index for each metric

Winter Precipitation (cm) ^a			
	Coefficients	p-value	R^2
NAO			
Mean Monthly	0.2880	0.0847	0.0249
Maximum-Month	3.7964	0.3842	0.0064
Minimum-Month	1.7181	0.2403	0.0116
PDO			
Mean Monthly	-0.4030	0.0285	0.0414
Maximum-Month	-5.6642	0.2447	0.0119
Minimum-Month	-2.8859	0.0797	0.0267
AMO			
Mean Monthly	0.1187	0.4553	0.0047
Maximum-Month	1.5710	0.7048	0.0012
Minimum-Month	0.3517	0.8006	0.0005

^a Highlighted values color key: Green, slope is consistent with hypotheses or p -value is less than 0.05. Yellow, p -value is close to 0.05 but slightly above. Red, slope is inconsistent with hypotheses or p -value is greater than 0.05 or adjusted R^2 value is less than 0.25.

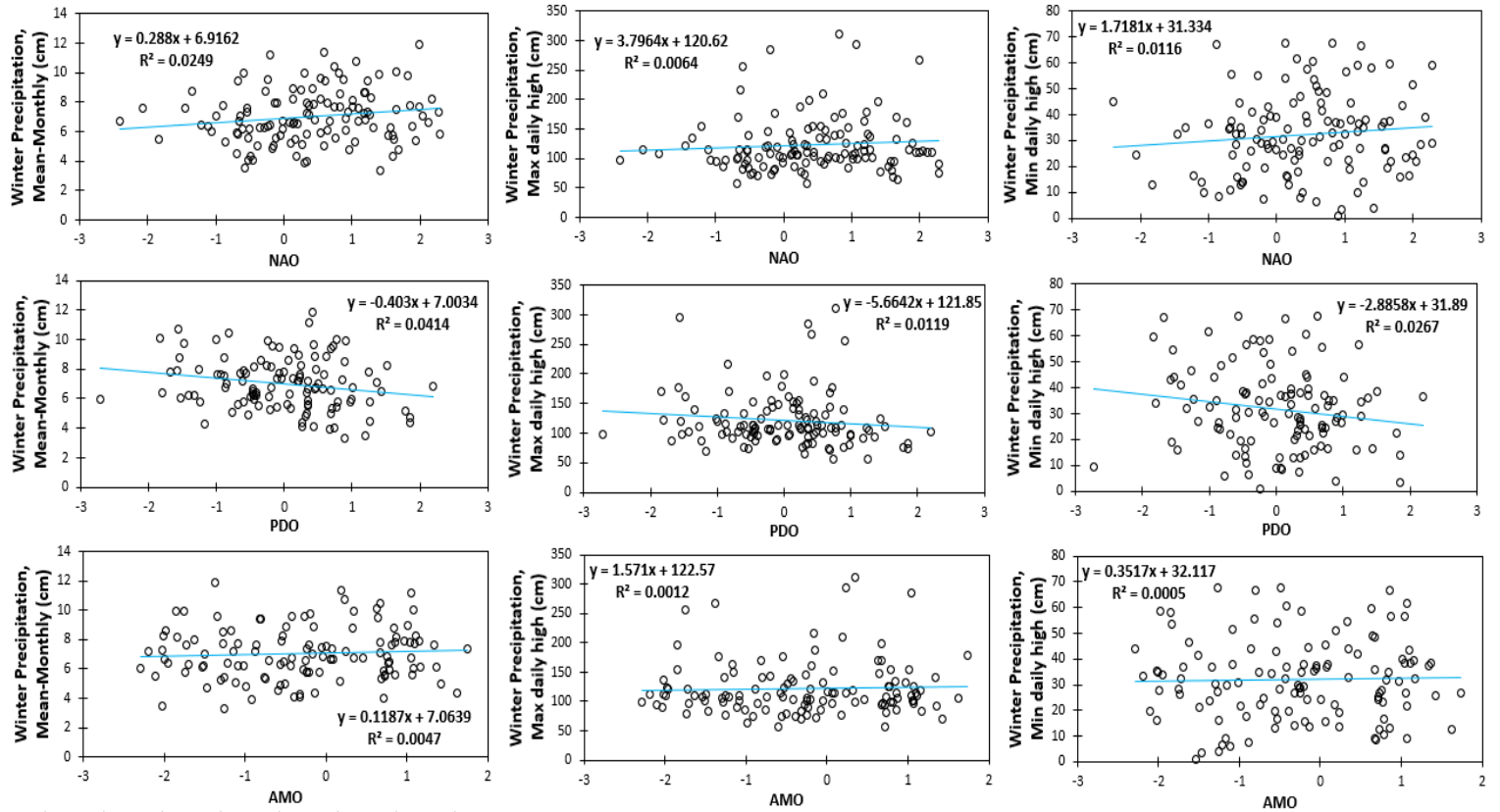


Figure 18. Linear regressions for each index individually (NAO in the first row, PDO in the second row, and AMO in the third row) against each of the metrics chosen (mean-monthly winter precipitation in first column, Maximum-month precipitation in the second column, Minimum-month precipitation in the third column).

V.C. Multiple regression with four indices

The results of the multiple regression analysis on precipitation using the indices MEI, NAO, PDO and AMO are given in Table 17. Only the mean-monthly metric was significant ($p=0.018$), explaining about 7% of the variance in precipitation. When only considering MEI, the R^2 was 0.03 (Ritzi et al., 2021), but in including all four perturbations the R^2_a became 0.07. Thus, more variance in winter precipitation is explained by the multivariate model, although the increase is small. The NAO and PDO indices in this model are the only ones that are significant at the $p = 0.023$, and $p = 0.025$ levels, respectively.

Table 17. Multiple regression on precipitation (cm) for each metric without interaction terms (n=116).

Winter Precipitation (cm) ^a						
Terms	Mean Monthly		Maximum Month		Minimum Month	
	<u>coefficient</u>	<u>p-value</u>	<u>coefficient</u>	<u>p-value</u>	<u>coefficient</u>	<u>p-value</u>
Intercept	6.922	< 2E-16	120.9	< 2E-16	31.27	< 2E-16
MEI	-0.338	0.1037	-5.448	0.334	-1.019	0.591
NAO	0.385	0.0232	4.972	0.278	2.170	0.161
PDO	-0.243	0.0250	-2.996	0.603	-2.487	0.202
AMO	1.228	0.1832	17.75	0.480	4.260	0.614
R^2_a	0.069		-0.006		0.010	
p-value	0.018		0.511		0.274	

^a Highlighted values color key: Green, p-value is less than 0.05 or R^2_a is greater than or equal to 0.25. Yellow, p-value is close to 0.05 but slightly above or R^2 is close to 0.25. Red, p-value is greater than 0.05 or adjusted R^2 value is much less than 0.25.

V.D. Multiple regression with four indices and interactions

The multiple regression including terms for interactions between each index on precipitation was not found to increase the R^2_a value and does not lead to a more significant model of precipitation. An example of a model that includes all 2, 3, and 4-way interaction terms against precipitation is shown in Table 18 and indicates that none of the interaction terms are statistically significant (p-value \leq 0.05). After the four-way interaction term was deemed not significant, it was removed, and only the 3-way interaction terms were considered. Furthermore, once they were deemed not significant, they were also removed, and only 2-way interaction terms were considered. The sequential removal of the highest order interaction terms did not lead to a more significant model for precipitation and does not support the hypothesis that the interactions between perturbations create statistically significant anomalies in winter precipitation at the study area.

Table 18. All 1, 2, 3, and 4-way interaction effects for each metric ($n=116$)

Winter Precipitation (cm) ^a						
Terms	Mean Monthly		Maximum Month		Minimum Month	
	coefficient	p-value	coefficient	p-value	coefficient	p-value
Intercept	6.989	<2E-16	123.75	<2E-16	31.990	<2E-16
MEI	-0.349	0.182	-3.700	0.606	-1.006	0.674
NAO	0.333	0.098	4.617	0.404	2.440	0.187
PDO	-0.410	0.095	-8.153	0.228	-1.728	0.442
AMO	0.314	0.816	-9.882	0.790	-1.746	0.888
MEI: NAO	-0.045	0.837	-6.929	0.256	2.359	0.246
MEI: PDO	-0.161	0.470	-5.930	0.337	-1.293	0.529
MEI: AMO	0.412	0.785	5.312	0.899	0.774	0.956
NAO: PDO	0.031	0.893	3.380	0.594	-2.106	0.320
NAO: AMO	-0.073	0.954	21.758	0.531	4.813	0.678
PDO: AMO	-0.542	0.740	-19.095	0.672	13.111	0.384
MEI: NAO: PDO	0.111	0.557	4.792	0.362	-1.267	0.469
MEI: NAO: AMO	0.155	0.906	-15.907	0.661	10.050	0.406
MEI: PDO: AMO	1.779	0.218	35.087	0.378	4.994	0.706
NAO: PDO: AMO	-1.384	0.412	-20.102	0.666	-0.749	0.962
MEI: NAO: PDO: AMO	1.268	0.296	11.323	0.735	4.777	0.668
R^2_a	0.054		-0.045		-0.009	
p -value	0.145		0.811		0.530	

^a Highlighted values color key: Green, p-value is less than 0.05 or R^2_a is greater than or equal to 0.25. Yellow, p-value is close to 0.05 but slightly above or R^2 is close to 0.25. Red, p-value is greater than 0.05 or adjusted R^2 value is much less than 0.25. Gray, regression term is already being expressed in the highest order interaction terms and is not considered as supporting or rejecting the hypothesis here.

VI. DISCUSSION

VI.A. Temperature

Ritzi et al. (2021) found that essentially none of the variance ($R^2 = 2E-9$) in winter temperature was explained by MEI as a predictor variable in the regression. By here including indices for other ocean-atmospheric perturbations (NAO, PDO, AMO), 25% of the variance in winter temperature was explained. The NAO index is the most significant variable to come out of the multiple regression (p -value = $1.8E-6$). These results are consistent with the results of other studies that have recognized the NAO perturbation as a useful predictor for temperature and those that consider it the most important pattern of atmospheric variability in the Northern Hemisphere (Hurrell, 1995; Li et al., 2013). However, most of these studies are limited to the hydrologic effects in the eastern U.S. and Europe (Lindsey et al., 2009; Seager et al., 2010; Lindsey, 2011), whereas this study highlights the importance of NAO on winter temperature in Southwest Ohio. These results are also consistent with Balvanz et al. (2017) more local study, which showed a negative correlation between the NAO index and snowfall from 11 stations within the Midwest.

Also, in considering the additive effect of all four ocean-atmospheric phenomena on temperature, the variance explained by the mean monthly metric increases from 14% (with NAO alone) to 23%. Indicating, a model incorporating a single teleconnection pattern will not explain as much variance in temperature as a model that includes multiple teleconnection patterns.

Furthermore, when the interactions between variables were added to the regression, and all 3-way interactions with NAO included were accounted for, only the 3-way interaction between NAO, MEI, and PDO was significant (p -value = 0.043), with the adjusted $R^2 = 0.25$ for the mean-monthly metric. The increase in variance explained by the model with interactions as

compared to the model without interactions is small (2% increase), but the statistically significant 3-way interaction term between NAO, MEI, and PDO is worth exploring.

In considering whether these three indices are in a positive or negative phase, and the 8 possible combinations of the index states between them, it was found that when NAO is negative, but MEI and PDO are both positive (Combination 4) the mean winter temperature was statistically significantly about 1 °C lower (p -value ~ 0.0076) on average than in other years on record. Conversely, when NAO is positive, but MEI and PDO are both negative (Combination 6) the mean winter temperature was statistically significantly about 1 °C higher (p -value ~ 0.0041) on average than in other years on record. Also, when NAO and MEI are both negative, but PDO is positive (Combination 8) the mean was statistically significantly about 0.85 °C lower (p -value ~ 0.034) on average than in other years on record. In the multiple comparison, only the comparison between combinations 6 and 4 were statistically significant with a p -value = 0.02, indicating winters under combination 6 were on average 1.73 °C warmer than winters under combination 4.

These results are consistent with the knowledge that the NAO index is a dominant perturbation in the Northern Hemisphere circulation since it is considered the most significant variable to come from the regression analyses of temperature, considering its relative proximity to the study area, and relationship with the polar jet stream (Figure 10 and 11; Hurrell, 1995; Lindsey et al., 2009; Kennedy et al., 2014), but it is interesting that the effect on temperature seems to be more pronounced when the MEI and PDO indices are opposite of the NAO index, considering the positive/negative phases of the MEI and PDO indices individually were hypothesized to affect temperature in a similar way as the NAO phases (Figure 13; Ropelewski et al., 1987, 1989; Hurrell, 1995; Mantua et al., 1997; NOAA CPC, 2012; Kennedy et al., 2014;

Lindsey, 2016; 2017). This would imply that when the waters of the eastern equatorial Pacific and northern Pacific coasts are anomalously warmer (i.e., El Niño and positive PDO; Figure 8a), and the pressure differential between the Icelandic low and Azores high is small (negative NAO; weaker westerlies/less-stable polar vortex), southwestern Ohio observes around 1 °C colder temperature most of the time (83%). Conversely, when the waters of the eastern equatorial Pacific and northern Pacific coast are cooler (i.e., La Niña and negative PDO; Figure 8d), and the pressure differential between the Icelandic low and Azores high is large (positive NAO; stronger westerlies/more-stable polar vortex), Southwestern Ohio observes around 1 °C warmer than average temperatures most of the time (71%).

This may indicate that the polar jet stream is likely to stay north of southwest Ohio, and the Pacific jet stream may move up into the Midwest when the NAO index is positive and the MEI and PDO indices are negative. Conversely, this may also conclude that when the NAO index is negative and the MEI and PDO indices are positive the polar jet stream is more likely to drop down as low as southwest Ohio and the Pacific jet stream may stay farther south of the Midwest. This hypothesis could be the premise of furthering research in the atmospheric sciences in future studies.

VI.B. Precipitation

Ritzi et al. (2021) found that El Niño winters had statistically-significantly less precipitation. However, ENSO cycles only explained 3% of the variance in precipitation. The results for each individual perturbation added in this study (NAO, PDO, AMO) have either an inconsistent slope, p -value above 0.05, or a negligible R^2 value, and do not support the respective hypothesis for an effect associated with those perturbations. However, including MEI with NAO, PDO, and AMO in the regression model here gave a slight increase in the variance explained from 3% (with

ENSO alone) to 7%. In this multivariate model only the PDO and NAO indices had p-values below 0.05. These results give evidence that the influences of NAO, ENSO, PDO, and AMO on precipitation were much less than their influences on temperature, if influences exist.

VI.C. Implications

Those involved in agriculture, in water management, in understanding ecological stressors caused by changes in temperature and precipitation in Ohio, or any other activity aided by weather forecasting may benefit if knowing the NAO, ENSO and PDO conditions in late fall has predicative implications for the ensuing winter weather. For example, one of the most common natural disasters across the globe are floods (Emerton et al., 2016), and therefore accurate flood forecasting is of high importance. For example, the Miami Conservancy District (MCD) protects communities of Southwest Ohio from flooding through maintaining dams and levees and monitoring water levels. When winter temperatures are lower than usual, the ground is more likely to freeze, which can lead to increased runoff into the rivers (Niu et al., 2006), and when winter precipitation is higher than usual, it can lead to an increased snowmelt in the spring. In either case, the MCD would benefit from knowing information gathered from this research. Furthermore, improved predictions of temperature and precipitation can improve farming practices in an agricultural society, and hopefully lead to increased crop yield or less costly crop management.

VI.D. Future Work

In the future, studies expanding the geographic scope to more locations could answer questions like what the geographical extent of these weather anomalies is. For example, the USHCN has collected a century worth of precipitation and temperature records from several stations in Kentucky and Michigan that would allow for discerning if the results of this study are only locally existent, or if similar patterns extend into areas surrounding Southwestern Ohio.

Also, studies that consider the changing behavior of these ocean-atmospheric perturbations could determine how these anomalies change with the altering of these ocean-atmospheric phenomena over time. For instance, Capotondi et al. (2015) looked at the differing ENSO patterns and grouped years with eastern Pacific (EP) anomalies against years with central Pacific (CP) anomalies. By separating ENSO into CP-El Nino/La Nina and EP-El Nino/La Nina one could look for differences in the observed weather patterns and associated hydrologic effect. Furthermore, the results from this study statistically support the existence of some teleconnections and gives motivation for more work in the atmospheric sciences on the actual physical mechanisms, which may explain why NAO affects temperature but not precipitation in the study area. Clearly there is still much work that needs to be done in exploring how these teleconnection patterns have changed, are changing, and will change, not only globally but in specific watersheds as well, so more informed decisions about water management, agricultural use, and weather forecasting can be made.

VII. CONCLUSIONS

Winter temperature and precipitation in Southwest Ohio from 121 winters between 1896 and 2016 were examined for anomalies attributable to teleconnections with large scale atmospheric perturbations caused by the El Niño Southern Oscillation (ENSO), North Atlantic Oscillation (NAO), Pacific Decadal Oscillation (PDO), and the Atlantic Multidecadal Oscillation (AMO). The record of winter temperature gives evidence of a teleconnection with the NAO, ENSO, and PDO patterns, with the strongest link being for phases of the NAO (explaining 14% of variance alone). The majority of winters occurring during a positive-NAO-phase had mean monthly temperature warmer than the century long mean (CLM), and the majority of negative-NAO-phase winters had colder temperatures. The difference in temperature between positive and negative NAO phase winters was 0.82 °C, and the difference is statistically significantly different at the $p = 0.0005$ level. Furthermore, winters are increasingly warmer when NAO is increasingly positive and increasingly colder when NAO is increasingly negative (regression model with $p = E-5$). This teleconnection is the strongest when NAO is out of phase with ENSO and PDO. For example, the 21 winters when the NAO phase was positive and ENSO and PDO phases were negative (condition A) were 1.73 °C warmer on average than the 12 winters when NAO was negative and ENSO and PDO were positive (condition B), and the difference is statistically significantly different at the $p = 0.02$ level. The warmest winter on record (mean-monthly temperature of 6.9 °C) occurred under condition A, while the coldest (5.2 °C) occurred under condition B. Furthermore, it has been statistically significantly warmer most of the time (71%), by about 1 °C above normal during condition A, and about 1 °C colder most of the time (83%) during condition B, and the NAO, ENSO and PDO variations explain 25% of the overall variance in mean winter temperature (multi-regression model with $p = 0.02$). The mean winter temperature metric shows the largest effect, followed by the minimum-month metric, and the

maximum month metric shows the least effect. The record does not give evidence for an influence on winter temperature by the AMO.

Consistent with prior studies, mean monthly precipitation has been 5 cm less during El Nino events, with the decrease increasing with the strength of the El Nino, but a regression model for this influence only explains 3% of the variance in winter precipitation (Ritzi et al., 2021). Considering the additive effect of all four perturbations in the multi-regression model only slightly increased the variance explained to 7%. Thus, the record of winter precipitation during this time gives evidence that the influences of NAO, ENSO, PDO, and AMO on precipitation were much less than their influences on temperature, if influences exist.

REFERENCES

- Bai, X., J. Wang, C. Sellinger, A. Clites, and R. Assel (2012), Interannual variability of Great Lakes ice cover and its relationship to NAO and ENSO, *J. Geophys. Res.*, **117**, C03002, doi:10.1029/2010JC006932.
- Balvanz, A., Gallus, W., (2017). Effects of the North Atlantic Oscillation on Snow in the Midwest. Meteorology Senior Thesis. **20**. https://lib.dr.iastate.edu/mteor_theses/20
- Birkel, S. D., Mayewski, P. A., Maasch, K. A., Kurbatov, A. V, and Lyon, B., (2018), Evidence for a volcanic underpinning of the Atlantic multidecadal oscillation, *npj Clim. Atmos. Sci.*, **24**; doi:10.1038/s41612-018-0036-6
- Booth, R. K., Kutzbach, J. E., Hotchkiss, S. C., and Bryson, R. A., (2006), A reanalysis of the relationship between strong westerlies and precipitation in the Great Plains and Midwest regions of North America, *Climate Change*, **76**, 427–441, doi:10.1007/s10584-005-9004-3
- Börgel, F., Frauen, C., Neumann, T. and Markus Meier, H. E. (2020). The Atlantic Multidecadal Oscillation controls the impact of the North Atlantic Oscillation on North European climate. *Environmental research letters*, **15**(10), s. 104025, doi:10.1088/1748-9326/aba925
- Budikova, D., (2005), Impact of the Pacific Decadal Oscillation on relationships between temperature and the Arctic Oscillation in the USA in winter, *Clim. Res.*, **1** (29), 199–208
- Capotondi, A., Wittenberg, A. T., Newman, M., Lorenzo, E. D., Yu, J., Braconnot, P., Cole, J., Dewitte, B., Giese, B., Guilyardi, E., Jin, F., Karnauskas, K., Kirtman, B., Lee, T.,

- Schneider, N., Xue, Y., and Yeh, S. (2015). Understanding ENSO Diversity. *Bull. Am. Meteorol. Soc.*, **96**(6), 921–938. Doi:10.1175/BAMS-D-13-00117.1
- Cohen, J. (1988). Statistical power analysis for the behavioral sciences. 2nd ed. Hillsdale, NJ: Lawrence Erlbaum Associates, 400 p., ISBN 13: 9780805802832.
- Davini, P., Hardenberg, J. V., and Corti, S., (2015), Tropical origin for the impacts of the Atlantic Multidecadal Variability on the Euro-Atlantic climate, *Environ. Res. Lett.*, **10**, 094010, doi:10.1088/1748-9326/10/9/094010
- Emerton, R. E., Stephens, E. M., Pappenberger, F., Pagano, T. C., Weerts, A. H., Wood, A. W., Salamon, P., Brown, J. D., Hjerdt, N., Donnelly, C., Baugh, C. A., and Cloke, H. L., (2016), *WIREs Water*, **3**, 391–418. doi: 10.1002/wat2.1137
- Enfield, D. B., Mestas-Nuñez, A. M. and Trimble, P. J. (2001). The Atlantic Multidecadal Oscillation and its relation to rainfall and river flows in the continental U.S.. *Geophysical research letters*, **28**(10), s. 2077–2080. doi:10.1029/2000gl012745.
- Feldstein, S. B., (2000), The timescale, power spectra, and climate noise properties of teleconnection patterns. *J. Clim.*, **13**, 4430–4440.
- Feldstein, S. B., (2003), The dynamics of NAO teleconnection pattern growth and decay. *Q. J. R. Meteorol. Soc.*, **129**, 901–924.
- Felis, T., Merkel, U., Asami, R., Deschamps, P., Hathorne, E. C., Kölling, M., Bard, E., Cabioch, G., Durand, N., Prange, M., Schulz, M., Cahyarini, S. Y., and Pfeiffer, M., (2012), Pronounced interannual variability in tropical South Pacific temperatures during Heinrich Stadial 1, *Nat. Commun.*, **3** (965), doi:10.1038/ncomms1973

- Feng, Y., Chen, X., and Tung, K., (2020), ENSO diversity and the recent appearance of Central Pacific ENSO, *Clim. Dyn.*, **54**, 413–433, <https://doi.org/10.1007/s00382-019-05005-7>
- Gabric, L., Keeney, H. J., Pytlak, E. S., [date unknown], Climatological effects of the El Niño-Southern Oscillation in the lower Great Lakes and Ohio Valley, NOAA, National Weather Service, Cleveland (OH) Weather Forecast Office: El Niño & the Lower Great Lakes and Ohio Valley.
- Garrison, T., (2010). *Oceanography An Invitation to Marine Science*, 7th Ed., Belmont, CA: Brooks/Cole, 2010.
- Hall, R., Erdélyi, R., Hanna, E., Jones, J. M., and Scaife, A. A. (2015). Drivers of North Atlantic Polar Front jet stream variability. *Int J Climatol.*, **35**, 1697–1720 doi:10.1002/joc.4121
- Haynes, W., (2013), Tukey’s Test. In: Dubitzky, W., Wolkenhauer, O., Cho, K. H., and Yokota, H., (eds) *Encyclopedia of Systems Biology*. Springer, New York, NY.
https://doi.org/10.1007/978-1-4419-9863-7_1212
- Held, I. M., and Hou, A. Y. (1980). Nonlinear Axially Symmetric Circulations in a Nearly Inviscid Atmosphere. *J. Atmos. Sci.*, **37**, 515–533
- Hoskins B. J., and Valdes P. J., (1990). On the existence of storm tracks. *J. Atmos. Sci.*, **47**, 1854–1864
- Hurrell, J. W. (1995). Decadal Trends in the North Atlantic Oscillation: Regional Temperatures and Precipitation. *Science*, **269**, 676–679. <https://www.jstor.org/stable/2888966>

- Johnson, Z. F., Chikamoto, Y., Wang, S. Y., McPhaden, M. J., and Mochizuki, T. (2020). Pacific decadal oscillation remotely forced by the equatorial Pacific and the Atlantic Oceans. *Clim. Dyn.*, **55**, 789–811 <https://doi.org/10.1007/s00382-020-05295-2>
- Kennedy, C. and Lindsey, R. (2014) How is the polar vortex related to the Arctic Oscillation? NOAA, <https://www.climate.gov/news-features/event-tracker/how-polar-vortex-related-arctic-oscillation>
- Kerr, R. A., (2000), A North Atlantic climate pacemaker for the centuries, *Science*, **288**, 1984–1985
- Knight, J. R., Folland, C. K. and Scaife, A. A. (2006). Climate impacts of the Atlantic Multidecadal Oscillation. *Geophysical research letters*, **33**(17).
doi:10.1029/2006gl026242
- Kutner, M. H., Nachtsheim, C. T., Neter, J., Li, W., (2013), Applied Linear Statistical Models, 5th Ed., India, McGraw Hill, 2013.
- Kwon, Y.-H., Seo, H., Ummenhofer, C. C., and Joyce, T. M., (2020), Impact of Multidecadal Variability in Atlantic SST on Winter Atmospheric Blocking, *J. Clim.*, **33**, 867–892.
- Li, J., Sun, C., and Jin, F., (2013), NAO implicated as a predictor of Northern Hemisphere mean temperature multidecadal variability, *Geophys. Res. Lett.*, **40**, 5497–5502.
- Liberto, T. D. (2016). Going out for ice cream: a first date with the Pacific Decadal Oscillation, NOAA, <https://www.climate.gov/news-features/blogs/enso/going-out-ice-cream-first-date-Pacific-decadal-oscillation>

Lindsey, R. and Dahlman, L. (2009). Climate Variability: North Atlantic Oscillation, NOAA, <https://www.climate.gov/news-features/understanding-climate/climate-variability-north-atlantic-oscillation>

Lindsey, R. (2011). Winter Temperatures Influenced by North Atlantic Oscillation, La Niña. NOAA, <https://www.climate.gov/news-features/event-tracker/winter-temperatures-influenced-north-atlantic-oscillation-la-niña>

Lindsey, R., (2016), Climate variability: oceanic Niño index, NOAA, <https://www.climate.gov/news-features/understanding-climate/climate-variability-oceanic-niño-index>

Lindsey, R. (2017). How El Niño and La Niña affect the winter jet stream and U.S. climate. NOAA, <https://www.climate.gov/news-features/featured-images/how-el-niño-and-la-niña-affect-winter-jet-stream-and-us-climate>

Lindsey, R. (2021). Understanding the Arctic Polar Vortex. NOAA, <https://www.climate.gov/news-features/understanding-climate/understanding-arctic-polar-vortex>

Manney, G. L., Hegglin, M. I., Daffer, W. H., Schwartz, M. J., Santee, M. L., and Pawson, S., (2014), *J. Clim.*, **27**, 3248–3271.

Mantua, N.J., Hare, S.R., Zhang, Y., Wallace, J.M., and Francis, R.C., 1997. A Pacific interdecadal climate oscillation with impacts on salmon production. *Bull. Am. Meteorol. Soc.* **78**(6), 1069–1080.

Mantua, N. J. and Hare, S. R. (2002). The Pacific Decadal Oscillation. *J. Oceanogr.*, **58**, 35–44.

- Mccabe, G. J., Palecki, M. A. and Betancourt, J. L. (2004). Pacific and Atlantic Ocean influences on multidecadal drought frequency in the United States. *Proceedings of the national academy of sciences*, **101**(12), s. 4136–4141. doi:10.1073/pnas.0306738101
- Mitra, S., Srivastava, P., Singh, S., Yates, D., (2014), Effect of ENSO induced climate variability on groundwater levels in the lower Apalachicola-Chattahoochee-Flint River Basin, *Trans. ASABE*, **57**(5), 1393–1403. <https://doi.org/10.13031/trans.57.10748>
- Newman, M., Alexander, M. A., Ault, T. R., Cobb, K. M., Deser, C., Lorenzo, E. D., Mantua, N. J., Miller, A. J., Minobe, S., Nakamura, H., Schneider, N., Vimont, D. J., Phillips, A. S., Scott, J. D., and Smith, C. A., (2016), The Pacific Decadal Oscillation, Revisited, *Bull. Amer. Meteor. Soc.*, **29**, 4399–4427, doi:10.1175/JCLI-D-15-0508.1
- Nigam, S., and Baxter, S., (2015), Teleconnections. In: Encyclopedia of Atmospheric Sciences, Elsevier, Amsterdam, 90–109, <https://doi.org/10.1016/B978-0-12-382225-3.00400-X>
- Niu, G., and Yang, Z., (2006), Effects of Frozen Soil on Snowmelt Runoff and Soil Water Storage at a Continental Scale, *J. Hydrometeorol.*, **7**(5), 937–952.
- [NOAA CPC] NOAA Climate Prediction Center, 2012, North Atlantic Oscillation (NAO) [NOAA Online Webpage] [Accessed 2022 April 3].
<https://www.cpc.ncep.noaa.gov/data/teledoc/nao.shtml>
- [NOAA NCEI] NOAA National Centers for Environmental Information. [date unknown a]. Climate Data Online (CDO) [NOAA online database]. [accessed 2021 Feb 18].
<https://www.ncdc.noaa.gov/cdo-web/>

[NOAA NCEI] NOAA National Centers for Environmental Information. [date unknown b]. U.S. Historical Climatology Network (USHCN) [NOAA online database]. [Accessed 2022 April 3]. <https://www.ncei.noaa.gov/products/land-based-station/us-historical-climatology-network>

[NOAA PSL] NOAA Physical Science Lab, [date unknown], AMO (Atlantic Multidecadal Oscillation) Index, [NOAA Online Database] [accessed 2022 April 3]. <https://psl.noaa.gov/data/timeseries/AMO/>

[NOAA PSL] NOAA Physical Science Lab, 2013, North Atlantic Oscillation (NAO), [NOAA Online Database] [accessed 2022 April 3]. https://psl.noaa.gov/gcos_wgsp/Timeseries/NAO/

[NOAA PSL] NOAA Physical Science Lab, 2018, Pacific Decadal Oscillation (PDO), [NOAA Online Database] [accessed 2022 April 3]. https://psl.noaa.gov/gcos_wgsp/Timeseries/PDO/

Panetta, R. L. and Held, I. M. (1988). Baroclinic eddy fluxes in a one-dimensional model of quasi-geostrophic turbulence. *J. Atmos. Sci.*, **45**(22): 3354–3365

Riehl, H., (1962), Jet Streams of the Atmosphere, Report No. 32, Department of Atmospheric Science, Colorado State University, Fort Collins, Colorado.

Ritzi, R. W., Jr., Roberson, L. M., and Bottomley, M., (2021), El Niño Southern Oscillation (1896 to 2016): Quantifying Effects on Winter Precipitation and Temperature in Southwest Ohio, USA, *Ohio J. Sci.*, **121**(2), 64–77.

- Ropelewski, C. F. and Halpert, M. S. (1987). Global and regional scale precipitation patterns associated with the El Niño/Southern Oscillation. *Mon. Weather Rev.*, **115**(8), 1606–1626.
- Ropelewski, C. F. and Halpert, M. S. (1989). Precipitation patterns associated with the high index phase of the Southern Oscillation. *Journal of climate*, **2**(3), 268–284.
- Seager, R., Y. Kushnir, J. Nakamura, M. Ting, and N. Naik (2010), Northern Hemisphere winter snow anomalies: ENSO, NAO and the winter of 2009/10, *Geophys. Res. Lett.*, **37**, L14703, doi:10.1029/2010GL043830
- Shapiro, M. A., and Hampel, T. (1986). The Arctic Tropopause Fold. *Mon. Weather Rev.*, **115**, 444–45453.
- Sung, M., An, S., Kim, B., and Woo, S., (2014), A physical mechanism of the precipitation dipole in the western United States based on PDO-storm track relationship, *Geophys. Res. Lett.*, **41**, 4719–4726, doi:10.1002/2014GL060711.
- Trenberth, K. E., Branstator, G. W., Karoly, D., Kumar, A., Lau, N.-C., and Ropelewski, C., (1998), *J. Geophys. Res.*, **103**, 14291–14324.
- Vose, R. S, Applequist, S., Squires, M., Durre, I., Menne, M. J., Williams, C. N., Jr., Fenimore, C., Gleason, K., and Arndt, D., (2014), Improved Historical Temperature and Precipitation Time Series for U.S. Climate Divisions, *J. Appl. Meteorol. Climatol.*, **53**, 1232–1251.
- Wallace, J. M., and Gutzler, D. S., (1980), Teleconnections in the Geopotential Height Field during the Northern Hemisphere Winter, *Mon. Weather. Rev.*, **109**, 784–812.

- Walker, G. T., E. W. Bliss, (1932), World Weather V. *Mem. Roy. Meteor. Soc.*, **4**, 53–84.
- Wanner, H., Brönnimann, S., Casty, C., Gyalistras, D., Luterbacher, J., Schmutz, C., Stephenson, D. B., and Xoplaki, E., (2001), North Atlantic Oscillation – Concepts and Studies. *Surveys in geophysics*, **22**(4), s. 321–381. doi:10.1023/a:1014217317898
- Williams G. P. (1988), The dynamical range of global circulations – I, *Clim. Dyn.*, **2**, 205–260.
- Wilson E. B., (1927), Probable inference, the law of succession, and statistical inference. *J. Am. Stat. Assoc.* **22**(158), 209–212, <https://doi.org/10.1080/01621459.1927.10502953>.
- Wolter, K., (2011), Extended Multivariate ENSO Index (MEI.ext), [NOAA webpage], Boulder (CO): NOAA Physical Sciences Laboratory (PSL). <https://psl.noaa.gov/enso/mei.ext/>
- Wolter, K., (2018), Multivariate ENSO Index (MEI). [NOAA webpage], Boulder (CO): NOAA Physical Sciences Laboratory (PSL). <https://psl.noaa.gov/enso/mei.old/mei.html>
- Woolings, T., (2022), What is the jet stream?, NOAA, <https://origin-east-01-drupal-climate.woc.noaa.gov/news-features/blogs/enso/what-jet-stream>
- Yang, S., Li, Z., Yu, J., Hu, X., Dong, W., and He, S., (2018), El Nino–Southern Oscillation and its impact in the changing climate, *Nat. Sci. Rev.*, **5**, 840–857.
- Zhao, H., and Wang, C., (2015), Interdecadal modulation on the relationship between ENSO and typhoon activity during the late season in the western North Pacific, *Clim. Dyn.*, doi:10.1007/s00382-015-2837-1
- Zhang, R., and Delworth, T. L. (2007). Impact of the Atlantic Multidecadal Oscillation on North Pacific climate variability. *Geophys. Res. Lett.*, **34**, L23708, doi:10.1029/2007GL031601

Zhang, Y., Wallace, J. M. and Battisti, D. S. (1997). ENSO-like Interdecadal Variability: 1900–93. *Journal of climate*, **10**(5), s. 1004–1020. doi:10.1175/1520-0442(1997)010<1004:eliv>2.0.co;2